Element Abundances in Nearby Galaxies

By DONALD R. GARNETT

Steward Observatory, University of Arizona, Tucson AZ 85721, USA

In these lectures I present a highly opinionated review of the observed patterns of metallicity and element abundance ratios in nearby spiral, irregular, and dwarf elliptical galaxies, with connection to a number of astrophysical issues associated with chemical evolution. I also discuss some of the observational and theoretical issues associated with measuring abundances in H II regions and gas and stellar surface densities in disk galaxies. Finally, I will outline a few open questions that deserve attention in future investigations.

1. Introduction

The measurement of element abundances in galaxies other than our own has a roughly forty-year history, beginning with early attempts to measure helium abundances in giant H II regions in the Magellanic Clouds and M33 (Aller & Faulkner 1962, Mathis 1962) and pioneering studies of heavy element abundances from forbidden lines in extragalactic H II regions (e.g. Peimbert & Spinrad 1970, Searle 1971, Searle & Sargent 1972). Since then this field has grown tremendously, with high quality oxygen abundance data in some 40 nearby spiral galaxies and more than 100 irregular and compact dwarf galaxies. The amount of data for other elements (C, N, Ne, S, and Ar) has also improved tremendously, thanks largely to improvements in visible-wavelength detectors and the launching of spacecraft observatories, such as *IUE*, *HST*, and *ISO*, which have opened up the UV and IR spectral regions for spectroscopy.

The direct importance of determining the distribution of metallicity and element abundance ratios in galaxies is the contribution these measurements make to chemical evolution, and by consequence the evolution of galaxies. The elements heavier than H and He in stars and the interstellar medium (ISM) are the accumulated product of previous generations of star formation. The overall metallicity (usually represented by O/H in H II regions/ISM, and by Fe/H in stars) is determined by the total amount of previous star formation. Element abundance ratios, particularly C/O, N/O, or s-process/Fe, track the relative contributions of low-mass stars and high-mass stars, incorporating information on the stellar initial mass function (IMF). The abundances can be affected by gas flows (infall, outflow, or internal flows). It is possible, with modeling, to infer important clues to the evolution of galaxies from abundance measurements.

Beyond galaxy evolution, abundance measurements provide important ancillary information relevant to other very important astrophysical problems, including:

- The dependence of the I(CO)/N(H_2) conversion on environment and metallicity, which is critical for determining the amount of molecular gas in galaxies.
- The metallicity dependence of the Cepheid period-luminosity relation, currently under debate with respect to the determination of the Hubble constant and the extragalactic distance scale.
- Understanding the color evolution of galaxies. Colors of composite stellar populations depend on both age and metallicity; metallicity measurements thus reduce degeneracies in the interpretation of colors.
- Stellar mass loss rates, particularly the radiatively-accelerated winds of O and Wolf-Rayet stars, likely depend on the metallicity of the individual stars.
- The cooling function of interstellar gas. Cooling of interstellar gas is generally domi-

nated by metals (ions of metals in X-ray and ionized gas, singly-ionized metals in neutral gas, and molecules other than H_2 in molecular clouds), so the thermal balance in the ISM is a function of metallicity, with obvious implications for the formation of stars and galaxies.

In any field of investigation, a few key questions arise which form a framework for specific studies. I formulate a few of them below.

(*a*) How do metallicity and element abundance ratios evolve within galaxies, and how do variations relate to the evolution of the gas content and stellar light?

(*b*) What galaxy properties determine the observed compositions of galaxies? How is metallicity affected by galaxy dynamics (interactions, gas flows, angular momentum evolution)?

(*c*) How did heavy elements get into the intergalactic medium (IGM)? Were they ejected from galaxies by supernova-driven winds, ejected in tidal streams during galaxy interactions and mergers, or did they come from the first, possibly pre-galactic, stars?

(*d*) How well do simulations of galaxy formation and evolution reproduce the observed metallicities and distribution of abundances in galaxies?

The purpose of these lectures is to review the results of a variety of element abundance studies in galaxies other than our own in the nearby universe. I will not try to be all-inclusive, as the field is vast. For example, I will not attempt to discuss abundances in elliptical galaxies in detail, as better experts have already written extensive reviews on the subject (e.g. Worthey 1998, Henry & Worthey 1999), nor will I say much about luminous IR starbursts or low surface brightness galaxies. Much of the methodology behind abundance measurements in stars and ionized gas will be covered in great detail in the lectures by Lambert, Langer, and Stasińska; I will not spend much time on these subjects, but will highlight points of contention or uncertainty where appropriate. Likewise, Matteucci will discuss chemical evolution modeling in detail, so I will use the observational results to highlight areas where the data shed light on physical evolution of galaxies.

2. Observational Methods for Measuring Abundances

2.1. *Spectroscopy of H II Regions and Planetary Nebulae*

Most of the information we have on abundances in spiral and irregular galaxies have come from spectroscopy of H II regions. This is logical since H II regions are luminous and have high surface brightness (in the emission lines) compared to individual stars in galaxies. One can think of an H II region as an efficient machine for converting the extreme ultraviolet radiation of a hot, massive star into a few narrow emission lines, leading to a very luminous object in the optical/IR bands. As a result, observations of H II regions have typically provided our first look at abundances within galaxies. Indeed, emission lines are now being used to probe the ISM of galaxies at redshifts greater than 2, as will be discussed by Pettini in these proceedings.

Elements that are readily observed in the visible spectrum of H II regions include O, N, Ne, S, and Ar. With the exception of O, all of these elements may have important ionization states that emit only in the ultraviolet or infrared (for example, Ne^{+}, N^{+2}, S^{+3}). If we add UV spectroscopy we can study C and Si. Figure 1 shows an HST spectrum of one H II region in the SMC, showing the rich variety of forbidden emission lines and H, He recombination lines in the UV and optical spectrum. Other abundant heavy elements (such as Fe or Mg) may be observed in photoionized nebulae. One must always keep in mind that many elements in the ISM are strongly depleted onto grains,

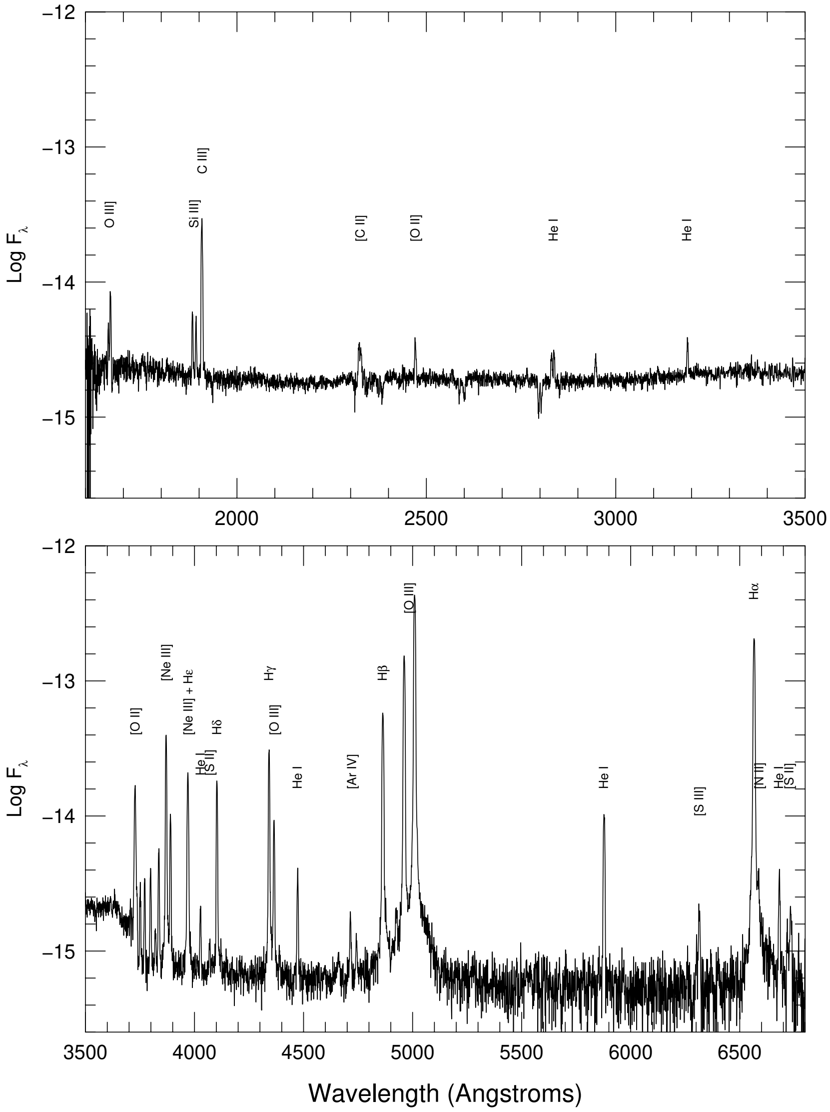

FIGURE 1. *Hubble Space Telescope* UV/optical spectrum of the H II region N88A in the Small Magellanic Cloud.

which affects the total abundance. This is an important but poorly known factor in many cases (such as O and C). Another caution is that H II regions show the composition of the present-day ISM, and are insensitive to the evolution of abundances with time.

Planetary nebulae (PNs) are essentially H II regions created by the ionization of a red giant envelope by the exposed hot stellar core, so spectroscopy of a PN provides information on a similar variety of elements as H II regions, with the same caveats. There are a number of significant differences, however. PNs are much less luminous than H II regions, so observations suitable for abundance measurements are restricted to the nearest galaxies; at the present time, measuring abundances in PNs is challenging in galaxies as close as M31 (Jacoby & Ciardullo 1999). Another difference is that the PN abundances are altered from the original stellar composition by nucleosynthesis – He, C, and N are often enriched, and even O may be affected. Thus, the use of PNs to measure abundances across galaxies must be pursued with caution. Nevertheless, measurements of PNs offer a means of measuring abundances across galaxies and their evolution over the range of ages of PN progenitors (a few tens to a few thousands of Myr). Stasińska will discuss PN abundance measurements in her lectures.

The observational and analytic techniques for determining abundances in H II regions have been discussed at great length by Skillman (1998) at the VIIIth Canary Island Winter School and by Stasińska in her lectures here. I will add a few remarks here on observing and deriving abundances.

2.1.1. *Observational Considerations*

It is easy to obtain a high-quality spectrum of an H II region in a nearby galaxy. It is not so easy to obtain a high-quality analysis afterward. Photon statistics is not the entire story in CCD spectroscopy. Additional random errors creep in during the flat-fielding and photometric calibration stages. It is difficult to flat-field a CCD frame to better than 1% even in imaging observations, where the most precise flat-fields involve matching the color of the target to that of the flat-field source (the night-sky for deep imaging – see Tyson 1986). Spectroscopists rarely observe such practices. In typical H II region spectroscopy, the flat-field is often obtained by combining an internal lamp to map the pixel-to-pixel sensitivity variations with a twilight sky observation to fit the slit vignetting. Both fill the slit in a different way than the object, which is an important consideration for the correction of interference fringing in the red. Flat-fields *repeatable* to 1% precision can be obtained over limited areas of a CCD spectrum, but the precision can be worse over regions where the lamp source is weak (in the blue part of the spectrum for example) or vignetting is strong.

The photometric calibration also contributes to the uncertainty of the measured spectrum. Flux standard stars are typically measured at widely spaced wavelengths (50 Å is common), and the sensitivity function of the instrument is determined by fitting a low-order polynomial or spline to the flux points. Such fits inevitably introduce low-order "wiggles" in the sensitivity function, which will vary from star to star. Based on experience, the best spectrophotometric calibration yield uncertainties in the *relative* fluxes of order 2-3% for widely-spaced emission lines; the errors may be better for ratios of lines closer than 20 Å apart. Absolute fluxes have much higher uncertainties, of course, especially for narrow-aperture observations of extended objects.

Another source of concern is the extended nature of H II regions and patchiness in interstellar reddening, which affects the measured line ratios. H II region spectra are often presented as integrated over the source. Reddening by dust is patchy everywhere we look, so the effects on the H II region spectrum must vary from point-to-point if we look at the spatial distribution. Although the spectrum of an H II region may be dominated by the areas with the highest surface brightness, it may be possible for a bright but obscured area to be given low weight, or for a region with a lower-quality spectrum to have an inflated surface brightness because of poorly-measured extinction. Thus the patchy nature of dust reddening must introduce additional uncertainty into measured line ratios. Spatially-resolved measurements are encouraged whenever possible.

The highly opinionated point here is that anyone who presents measured emission line strengths with uncertainties of 1% or less is probably not adding in all the error sources. Five percent uncertainties are probably more realistic for the brightest emission lines observed. Note that this level of precision is more than adequate for abundance measurements for most astrophysical problems.

2.1.2. *The Direct Method*

Direct abundance measurements can be made when one is able to measure the faint emission lines which are important diagnostics of electron temperature, T_e. The abundance of any ion relative to H^+ derived from the ratio of the intensity of a transition λ to the intensity of Hβ is given by

$$\frac{N(X^{+i})}{N(H^+)} = \frac{I(\lambda)}{I(H\beta)} \frac{\epsilon(H\beta)}{\epsilon(\lambda)}, \tag{2.1}$$

where $\epsilon(\lambda)$ represents the volume emission coefficient for a given emission line λ. For collisionally-excited lines in the low-density limit, the analysis in section 5.9 of Osterbrock (1989) applies.

When T_e has been measured, the volume emission coefficient for a collisionally-excited line is given by

$$\epsilon(\lambda) = h\nu q_{coll}(\lambda) = \frac{hc}{\lambda}\; 8.63 \times 10^{-6} (\Omega/\omega_1) T_e^{-0.5} e^{-\chi/kT_e} \tag{2.2}$$

where Ω is the collision strength for the transition observed, ω_1 is the statistical weight of the lower level, and χ is the excitation energy of the upper level. Ω contains the physics in the calculation; it represents the electron-ion collision cross-section averaged over a Maxwellian distribution of electron velocities relative to the target ion at the relevant temperature. Thus Ω has a mild temperature dependence, which can introduce a trend in abundance ratios if not accounted for.

Note on collision strengths: the vast majority of these values are computed, not experimental. This does not mean that they have zero uncertainty! A recent example is given by the case of [S III] (Tayal & Gupta 1999). This new 27-state R-matrix calculation resulted in changes of approximately 30% in the collision strengths for optical and IR forbidden transitions from earlier calculations. This shows that even for commonly-observed ions the atomic data is still in a state of flux. Observers should take into account the probable uncertainty in atomic data when estimating errors in abundances.

Another thing to account for is the fact that ionized nebulae are not strictly isothermal. Because [O III] is usually the most efficient coolant, the thermal balance at any point in an H II region depends on the local abundance of O^{+2}, as well as the local radiation field. The *ion-weighted* electron temperature for a given ion can vary with respect to T(O III) in a predictable way (Garnett 1992), depending largely on the metallicity. Figure 2 shows a plot of measured electron temperatures for [O III], [S III], [O II], and [N II] compared with the relationships derived from model photoionized nebulae (solid lines). The measured temperatures show correlations which agree quite well with the model relations, although there is quite a bit of scatter in the [O II] temperatures, and there may be a slight offset between T[S III] and the predicted relation, which may be real or an observational artifact. These results indicate that the photoionization models provide a reliable predictor of the thermal properties of H II regions.

For recombination lines, the emission coefficient is given by

$$\epsilon(\lambda) = h\nu q_{rec}(\lambda) = \frac{hc}{\lambda}\; \alpha_{eff}(\lambda), \tag{2.3}$$

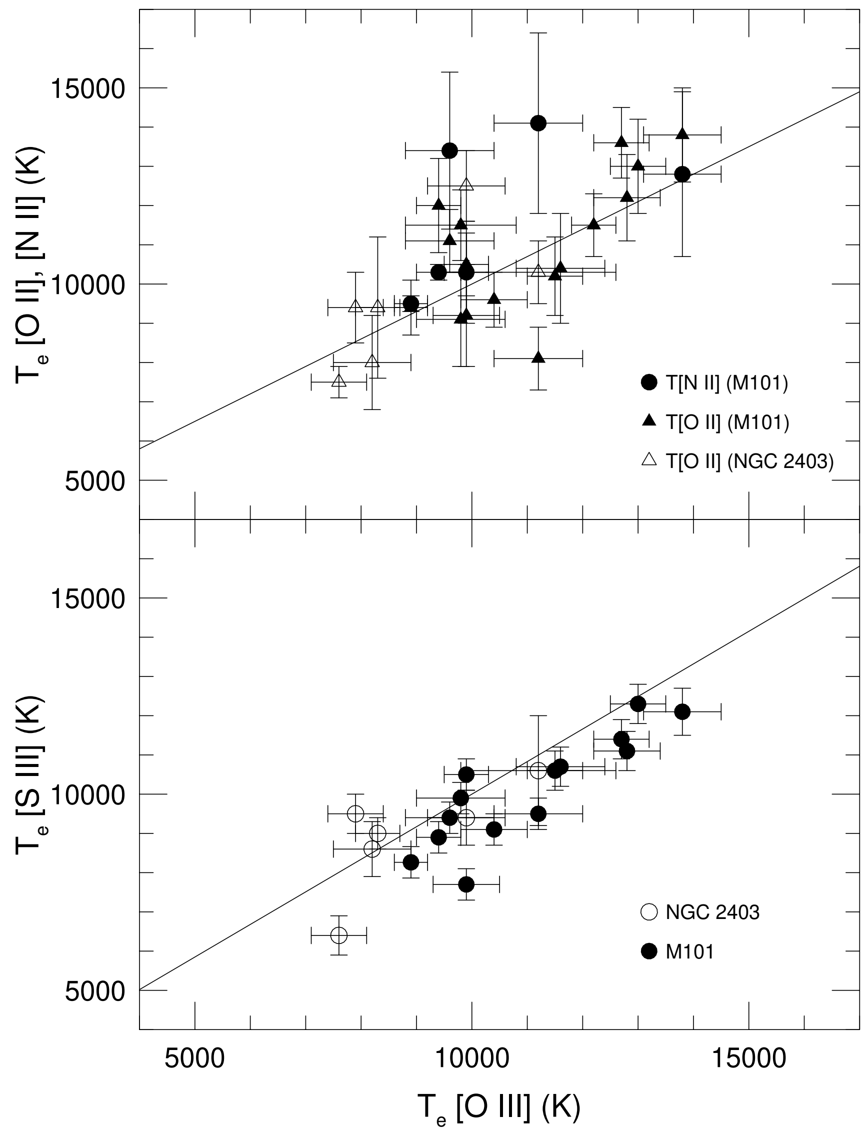

FIGURE 2. Comparison of electron temperatures derived from [O III], [O II], [N II], and [S III] measurements for H II regions in NGC 2403 and M101. The straight lines show the correlations predicted by photoionization models (Garnett 1992).

where $\alpha_{eff}(\lambda)$ is the "effective" recombination coefficient for the recombination line λ. α_{eff} incorporates the physics, including the cross-section for electron-ion recombination and the probability that a given recombination will produce the given emission line. α values for H vary as roughly T_e^{-1}; individual lines have mildly different T dependences, but recombination line ratios are only weakly dependent on T, and quite insensitive to n_e for densities less than 10^6 cm^{-3}.

Most astronomers are familiar with the bright H I Balmer and He I recombination lines in the optical spectrum of ionized nebulae. Heavier elements also emit a recombination spectrum, and O I, O II, C II, N I, N II and other permitted lines have been observed in PNs and the Orion Nebula. In principle, such recombination lines could yield more accurate abundances than the forbidden lines, because their emissivities all have roughly the same T dependence. In practice, the recombination lines scale roughly with element abundance, so even for O and C the RLs are typically fainter than 1% of Hβ, making them too faint to observe routinely in extragalactic H II regions. It is observed that recombination lines in some PNs give much higher abundances than the corresponding forbidden lines from the same ions (Liu et al. 1995, 2000; Garnett & Dinerstein 2001, 2002), and there is currently a raging debate over whether the recombination lines or the the forbidden lines provide more reliable abundances.

Measurements of infrared collisionally-excited fine-structure lines are gaining ground with the launch of the *ISO* spacecraft, and with the upcoming *SIRTF*, *SOFIA*, and *FIRST* missions. Recognizing that $\chi \approx$ 5-10 eV for UV forbidden lines, $\chi \approx$ 2-3 eV for optical forbidden lines, and $\chi < 0.2$ eV for IR fine structure lines with $\lambda > 7\mu$m, we see that the exponential term in Equation 2.2 goes to nearly unity, and the IR lines have a weak temperature dependence. Thus it should be possible to determine accurate abundances free of concerns over temperature fluctuations. One caveat is that the very important [O III] and [N III] fine-structure lines are sensitive to density, suffering from collisional de-excitation at $n_e \approx 1000$ cm^{-3}, so density fluctuations could introduce large uncertainties. Fine structure lines from Ne, S, and Ar in the 7-20μm range, however, are not so sensitive to density.

For extragalactic H II regions, the main limitations on IR observations so far have been small telescopes, high background, and short spacecraft lifetimes. Nevertheless, *ISO* is providing some information on H II regions in the Galaxy and other Local Group galaxies (and luminous starbursts), and the future missions promise even better data.

2.1.3. *"Empirical" (Strong-Line) Calibrations*

In many cases T_e can not be measured, either because the nebula is too faint or it is so cool that the temeprature-sensitive diagnostic lines (for example [O III] λ4363) are too weak. Thus, there is interest in having an abundance indicator that uses the strong forbidden lines.

Pagel et al. (1979) identified the line intensity ratio

$$R_{23} = \frac{I([O\ II]\lambda 3727) + I([O\ III]\lambda\lambda 4959, 5007)}{H\beta} \tag{2.4}$$

as an indicator of O/H in H II regions. They noted, based on a sample of extragalactic H II regions, that the measured T_e, O/H, and R_{23} were all correlated. This works because of the relationship between O/H and nebular cooling: the cooling in the ionized gas is dominated by emission in IR fine-structure lines (primarily the [O III] 52μm and 88μm lines), so as O/H increases, the nebula becomes cooler. In response, the optical forbidden lines, especially the [O III] lines, become weaker as O/H increases (excitation goes down as T decreases).

The R_{23} vs. O/H relation is fairly well calibrated empirically (based on abundances using the direct method) for log O/H between −3.5 and −4.0 (Edmunds & Pagel 1984). For higher O/H, the strong-line method breaks down because few measurements of T_e exist; only two measurements have been made for H II regions with roughly solar O/H

(Kinkel & Rosa 1994; Castellanos et al. 2001). In this regime, the relation has been calibrated using photoionization models (which I'll discuss later) that may have systematic errors. One other complication is that for log O/H < -3.8, the relation between R_{23} and O/H reverses, such that R_{23} decreases with decreasing abundance. The relation thus becomes double-valued, and at the turn-around region the uncertainties in O/H are much larger. This occurs because at very low metallicities the IR fine-structure lines no longer dominate the cooling because there are too few heavy elements. As a result the forbidden lines more directly reflect the abundances in the gas.

This double-valued nature of R_{23} has led some to seek other strong-line diagnostics. The ratio [O III]/[N II] (Alloin et al. 1979; Edmunds & Pagel 1984) has been promoted to break the degeneracy in R_{23}. This ratio does appear to vary monotonically with O/H, although the observational scatter generally is larger than for R_{23}. More recently, the emission line ratio

$$S_{23} = \frac{I([S\ II]\lambda\lambda 6717, 6731) + I([S\ III]\lambda\lambda 9069, 9532)}{H\beta} \tag{2.5}$$

has been calibrated as an indicator of O/H by Díaz & Pérez-Montero (2000). S_{23} has the advantage of varying monotically over the range $-4.3 <$ log O/H < -3.7 in which R_{23} becomes ambiguous. S_{23} does become double-valued for O/H > -3.4. Where this relation breaks down is uncertain at present because there are too few measurements. In addition, the ratio [N II]λ6583/Hα has been promoted as another possible measure of O/H (van Zee et al. 1998; Denicoló, Terlevich & Terlevich 2001). [N II]/Hα varies monotonically with O/H over the entire range over which it is calibrated, but the scatter is quite large, especially at low values of O/H in dwarf irregular galaxies. Note that S_{23} and [N II]/Hα are employed here as measures of the *oxygen* abundance, not sulfur or nitrogen and are calibrated by direct measurements of O/H. Thus, non-solar abundance ratios are not a concern.

At the same time, there are several limitations.

(*a*) None of these strong-line diagnostics is well calibrated for log O/H > -3.5. At higher metallicities, the calibration is largely derived from photoionization models.

(*b*) The accuracy of each of these calibrations is quite limited. For R_{23} the usual quoted uncertainty is ± 0.2 dex, which is roughly the scatter; in the turnaround region, the uncertainty is significantly larger. The accuracy of S_{23} is probably about the same; although there are few data points to pin down the scatter at the present time. The scatter in [N II]/Hα is significantly larger, about ± 0.3 dex; most of this scatter is real, not observational.

(*c*) The strong-line abundance relations are subject to systematic errors, because the forbidden-line strengths depend on the stellar effective temperature and ionization parameter as well as abundances. If a galaxy has a low star formation rate and only low-luminosity H II regions with cooler O stars, the empirical calibration could give a systematically different O/H than a galaxy with many of the most massive O stars and luminous giant H II regions.

2.1.4. *Photoionization Models*

Some have said that the use of photoionization models to estimate nebular abundances is the "last resort of scoundrels", so to speak. I admit that I have used photoionization models to commit offenses in the past. Since Grazyna Stasińska will cover the mechanics of photoionization modeling in detail in her lectures, I will confine my remarks to what I feel are major uncertainties and observational considerations that need to be addressed.

Gas-star geometry: This is an observational consideration, since the geometry influences the ionization parameter. The classical model of an H II region is a uniform sphere with a point source of ionizing photons. High-resolution images of real H II regions show that they are anything but this. The Orion Nebula is better modeled as a blister, with the brightest areas being the photoevaporating surface of molecular cloud. *Hubble Space Telescope* images of giant H II regions show them to resemble bubbles more than filled spheres, often with a surrounding halo of superbubbles. Young star clusters can often be found outside the main H II region associated with the superbubbles (Hunter et al. 1996). In many cases the ionizing cluster is not centrally condensed, but rather quite loose and extended (for example, NGC 604 and I Zw 18). Even the 30 Doradus nebula, which is dominated by the compact cluster R136a, also includes an extended distribution of O giants, supergiants and Wolf-Rayet stars, plus luminous embedded, possibly pre-main-sequence stars (see Walborn 1991, Bosch et al. 1999). To my knowledge, there has been no investigation of the effect of an extended distribution of ionizing sources on H II region spectra.

The effects of density and density variations are related to this problem. T_e, and thus the optical forbidden line strengths, are very sensitive to density because of collisional de-excitation of the far-IR fine structure cooling lines (Oey & Kennicutt 1993). This is most true for metal-rich H II regions, so, for example the relation between R_{23} and O/H from ionization models depends on the average density asssumed. It is not clear yet that observed integrated densities from, say, the [S II] line ratio accurately reflect mean densities. It is highly likely that a range of densities is more representative of nebular structure, although a functional form is not yet known.

A great deal of work needs to be done in this area.

Wolf-Rayet stars: There are a number of myths about Wolf-Rayet stars and their influence on the H II regions. The first myth is that the presence of Wolf-Rayet stars indicates an age of at least 3 Myr for the ionizing OB association, which is the result obtained from stellar evolution and spectrum synthesis modeling. However, this idea is demonstrated to be not true specifically in the case of 30 Doradus, which contains numerous W-R stars, yet has a color-magnitude age of 1.9 Myr (Hunter et al. 1995). This contradiction is the result of a new population of hydrogen-rich W-R stars noted by de Koter, Heap & Hubeny (1997). Thus we need to reconsider our ideas about using W-R stars to constrain the ages of stellar populations.

The second myth is that W-R stars add a hard component of photons with energies greater than 54 eV to the ionizing radiation field. Again, this is a result from the combination of stellar atmosphere models for Wolf-Rayet stars and spectrum synthesis models. The reality is that only about 1 in 100 W-R stars emits significant amounts of radiation beyond 54 eV. Those W-R stars that are associated with nebular He II emission in nearby galaxies tend to be rare high excitation WN and WO types (Garnett et al. 1991). X-ray binaries are also implicated in nebular He II emission (Pakull & Angebault 1986). We do not yet understand the evolutionary status of these stars, so it is premature to predict them from the stellar evolution models. Indeed, a comparison of photoionization models with the spectral sequence of H II regions indicates that OB cluster models that include such hot W-R stars produce results that are not consistent with observed emission-line trends (Bresolin, Kennicutt, & Garnett 1999).

It is not clear that we know very well at all the ionizing spectral energy distribution of Wolf-Rayet stars, or of O stars for that matter. Stellar atmosphere models which incorporate stellar winds, departures from LTE and plane-parallel geometry, and realistic opacities are still in the development stage, and the effective temperature scale of O stars is still in flux (Martins, Schaerer, & Hillier 2002).

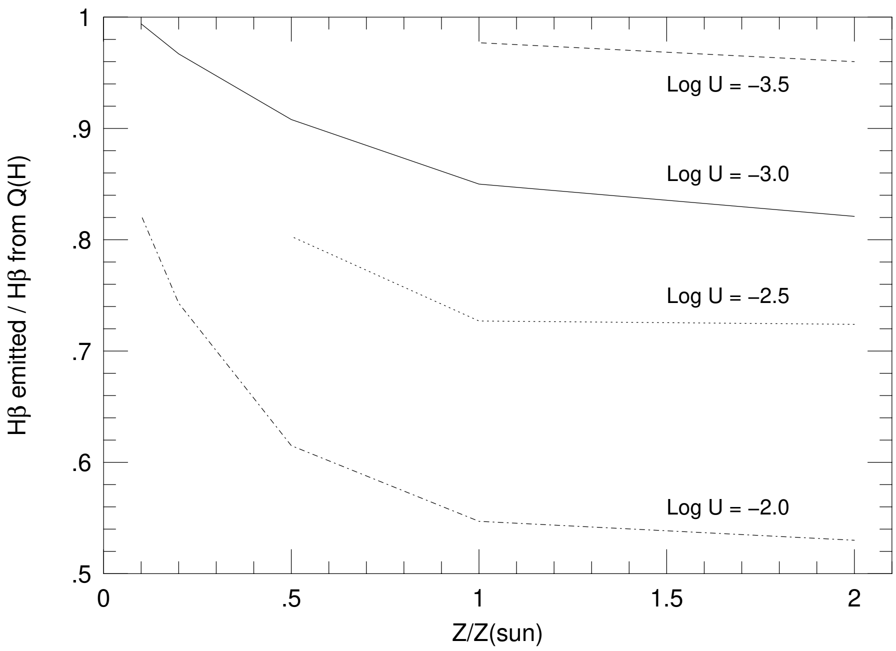

FIGURE 3. The ratio of emitted Hβ emission to that predicted from the stellar ionizing photon luminosity as a function of the nebular abundances, showing the effects of absorption of ionizing photons by dust grains. The models are for a stellar temperature of 40,000 K and assume a linear increase of the dust-to-gas ratio with metallicity. From Garnett (1999)

A great deal of work needs to be done in this area.

Dust: Dust has three major effects on the H II region spectrum. First, dust grains mixed with the ionized gas absorb Lyman-continuum radiation. Second, obscuration by dust is typically patchy; differential extinction between stars and gas can affect the emission line equivalent widths. Third, dust can affect the heating and cooling by emitting and recombining with photoelectrons.

The absorption cross-section for standard interstellar dust grains extends well into the EUV spectral region with a peak near 17 eV. Dust grains are thus quite capable of absorbing ionizing photons in the H II regions, and in fact can compete with H and He. When this occurs, the flux of Balmer line emission is reduced over the dust-free case. Figure 3 displays a set of ionization models showing the reduction in Hβ line emission over that expected from the number of ionizing photons for dusty H II regions. I have assumed standard interstellar grains (Martin & Rouleau 1990), with a dust-to-gas ratio that varies linearly with metallicity over the range 0.1-2.0 solar O/H. The models show that grains can reduce the emitted Hβ flux by as much as 50%. The amount lost depends strongly on the ionization parameter, increasing for higher ionization parameters. A region with high U is likely to be a young one where the gas is close to the star cluster; thus more Hβ photons are missed, and EW(Hβ) reduced the most, for the youngest clusters.

Incidentally, the same phenomenon leads one to underestimate the number of ionizing photons. Therefore, claims of leakage of ionizing photons from H II regions, based

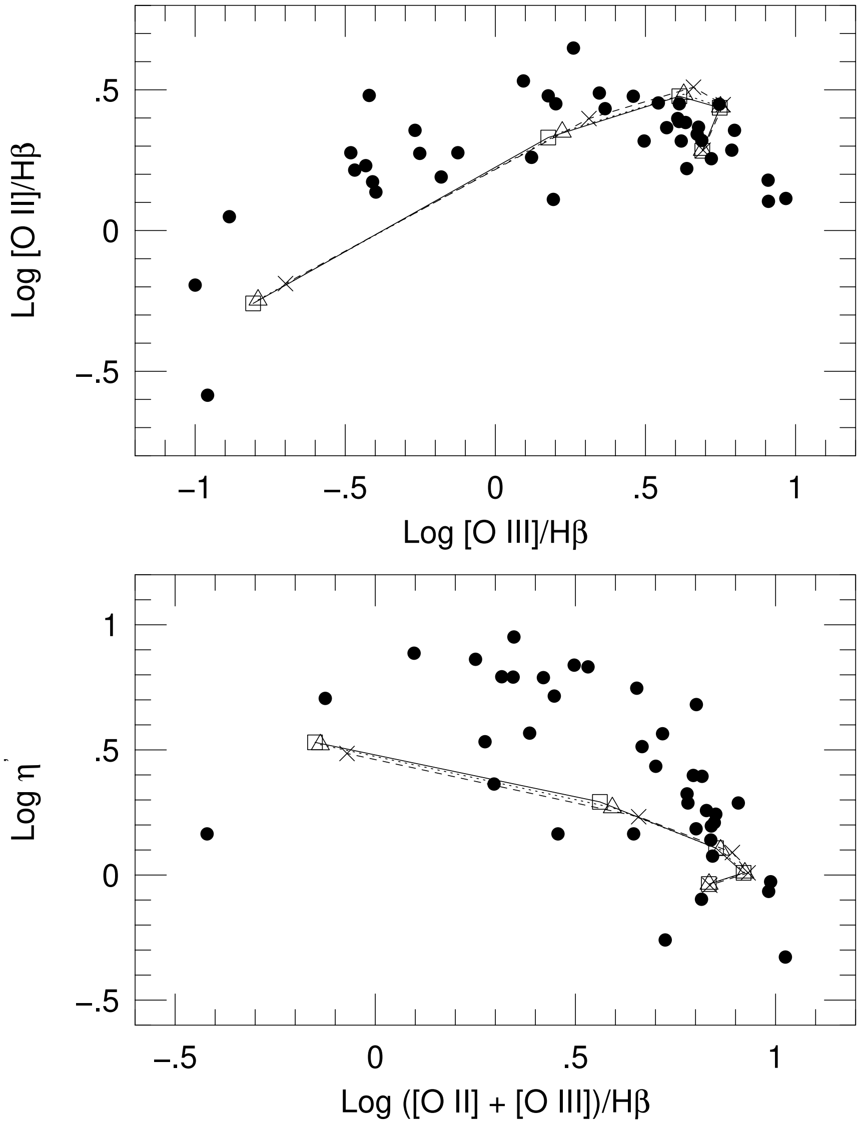

FIGURE 4. The effects of dust grains on forbidden-line strengths in H II regions. Three sequences of models are shown, with T_{eff} = 40,000 K and log $U = -3$. *Solid line plus squares:* dust-free models; *dashed line + crosses:* models with standard ISM grains; *dotted line plus triangles:* models with Orion-type grains. The effects of grains on the emission-line ratios are seen to be modest. From Garnett (1999)

on comparing N(Ly-c) from Balmer lines fluxs with that estimated from the OB star population, must be viewed with some skepticism.

Differential extinction between the stars and the gas can also affect EW(Hβ). Calzetti et al. (1994) found that the obscuration toward starburst clusters tended to be lower than that toward the ionized gas. They determined that, on average, A_V toward the stars was about one-half of that toward the gas. This is understandable if the stars have evacuated a cavity in the ionized gas through the combined effects of radiation pressure and stellar winds. The average derived obscuration for H II regions in spirals is $A_V \approx 1$ mag. If A_V(stars) is only 0.5 mag, then the observed EW(Hβ) will be about 40% lower than the intrinsic value.

These results suggest that dust effects can easily cause one to underestimate the intrinsic EW(Hβ), even for metallicities as low as 0.1 solar O/H. This would lead to a systematic bias toward larger ages for the stellar population. One should therefore exercise caution in weighting EW(Hβ) as a constraint on the synthesis models.

By contrast, the effects of dust on the relative forbidden-line strengths are modest (Figure 4), except at high metallicities (Shields & Kennicutt 1995). One exception is in the case of very hot ionizing stars (for example the central stars of planetary nebulae), where ionization of grains can lead to additional photoelectric heating of the nebula (e.g., Ferland 1998, Stasińska & Szczerba 2001).

A great deal of work is needed in this area.

Note on atomic data for ionization calculations: the vast majority of the values used for photoionization and recombination cross-sections are computed, not experimental. This does not mean that their uncertainties are zero! In fact, the best values are probably not accurate to better than 15-20%. Thus, it is unreasonable to expect photoionization models to match real H II region spectra to an accuracy much better than this.

2.2. *Spectroscopy of Individual Stars*

Stellar spectroscopy has been a very valuable tool for studying the composition and evolution of stars in our Galaxy. Recent improvements in instrumentation and the construction of 8-10m telescopes has allowed this kind of work to be extended to other galaxies. It is not possible yet to do routine spectroscopy of F and G main sequence stars outside the Milky Way, so these studies have concentrated on A and B type supergiants or red giants. Nevertheless, detailed abundance studies of individual stars is not likely to extend far beyond the Local Group for some time because of telescope size limitations.

The supergiants are an important complement to spectroscopy of H II regions, since they sample similar spatial and temporal distributions. Furthermore, they overlap in many of the elements that can be studied: C, N, O, Ne, and so on. On the one hand, the supergiants provide information on elements such as Si, Fe and s-process elements that are depleted into grains in the ISM. On the other hand, the H II regions provide a valuable comparison for He, C, and N which may be affected by internal mixing and nucleosynthesis in the massive stars, which is covered by Norbert Langer's contribution. This is one of the important uncertainties in abundance studies for these stars; others include the degree to which conditions depart from LTE, and the effects of spherical geometry and stellar winds.

Spectroscopy of red giants is well established from Milky Way studies, as discussed by David Lambert. Red giants are valuable because they sample abundances over long time spans, from a 100 Myr to greater than 10 Gyr. A wide variety of elements can be studied, including α capture elements, Fe-peak elements, and neutron-capture elements. C, N, and O (and s-process elements in AGB stars) can be affected by internal mixing. Since red giants are fainter than H II regions or supergiants, detailed spectroscopy is limited to the Milky Way's satellite galaxies at present.

For metallicity distributions, one can examine lower spectral resolution diagnostics.

The most useful of these has been the Ca II triplet indicator (Armandroff & Da Costa 1991), which uses the combined equivalent width of the Ca II triplet near 8500 Å, calibrated with metallicities of globular clusters, to infer the metallicity [Fe/H] (where the brackets denote the logarithmic abundance relative to that in the Sun). The main uncertainty of this method is that the Ca/Fe abundance ratio can vary depending on the star formation history, so the globular clusters may not provide the correct metallicity calibration for galaxies with a variety of star formation histories. Work needs to be done to calibrate the Ca II triplet with [Ca/H] rather than [Fe/H] to remove this ambiguity.

2.3. *Stellar Photometry and Color-Magnitude Diagrams*

Color-magnitude diagrams of galaxy populations can provide some information on the metallicity (or metallicity spread) of a stellar population, since features in the CMD, such as the color of the red giant branch, can vary with metallicity. Unfortunately, these features also vary with age of the populations, so there is a degeneracy between age and metallicity in the CMD (and in composite colors). Systematic uncertainties may also be introduced by variations in element abundance ratios and by reddening. Thus, color-magnitude diagrams are at best indicative of metallicities.

2.4. *Spectrum Synthesis of Stellar Populations*

Spectrum synthesis for deriving metallicities has been applied mostly to elliptical galaxies. Since I am not an expert on this, I refer the reader to Guy Worthey's review in Henry & Worthey (1999) and references therein for details. Needless to say, spectrum synthesis is an intricate and uncertain art; the results depend on the choices of spectral templates, element abundance ratios, and star formation histories. Worthey points out that 25 spectral indices are available to derive metallicities and ages for old stellar populations. (In 1986 there were 11 indices in the Lick spectral index system [Burstein, Faber, & González 1986].) Unfortunately, most of these vary in a degenerate way with age and metallicity of the stellar population. The best indices for breaking this degeneracy are (1) Hβ or a higher Balmer line, which are more sensitive to age; and (2) Fe4668 (which is actually a C_2 feature), more sensitive to metallicity. In addition, the Mg index (covering Mg b and Mg_2 features between 5150 and 5200 Å) provides information on Mg/Fe.

2.5. *Surface Photometry and Galaxy Colors*

Since the colors of stars are sensitive to both age and metallicity (as pointed out in Section 2.3 above) it is readily concluded that the colors of galaxies similarly depend on age and metallicity. The situation is a bit more complicated because in galaxies the colors represent composite stellar populations. A further complication is the ubiquitous presence of dust, which has a clumpy distribution mixed with the stars rather than a uniform screen. Nevertheless, the analysis of galaxy colors could provide a useful means of studying averaged ages and metallicities for stellar populations in very large samples of galaxies covering a wide range of redshifts, particularly galaxies that are too faint for spectroscopy.

As with stars, of course, a difficulty with using colors is that variations in age and metallicity cause similar variations in galaxy colors. This is especially true for optical colors, which have been known for some time to be almost completely degenerate with regard to variations in age and metallicity (see Figure 5). This degeneracy can be broken to a large extent by including IR photometry, particularly K-band surface photometry, as illustrated in Figure 6 from Bell & de Jong (2000). Bell & de Jong have exploited this property to derive *luminosity-weighted* mean ages and metallicities for a sample of low-inclination disk galaxies. Note that the luminosity weighting means that the

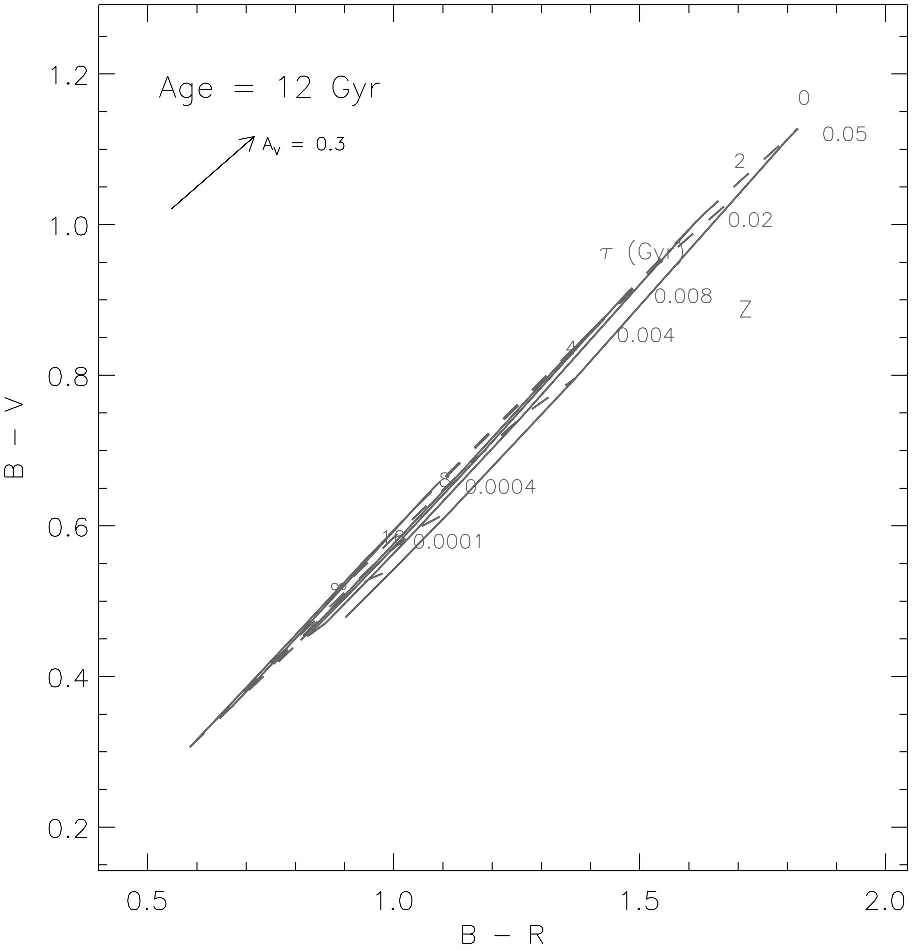

FIGURE 5. Synthetic B–R vs. B–V colors for disk galaxies based on population synthesis models. The colors are from Bruzual & Charlot models with an exponentially decaying star formation rate with timescale τ ranging from 0 Gyr to infinity and metallicity Z ranging from 0.0001 to 0.05; see Bell & de Jong (2000) for details of the models. Solid lines connect models of constant Z, while dashed lines connect models of constant τ. All galaxies start forming stars 12 Gyr ago. The effects of interstellar reddening by foreground screen with $A_V = 0.3$ magnitude is shown by the vector in the upper left corner. Diagram courtesy of Eric Bell.

derived properties do not represent the *present-day* metallicities, as the emission-line measurements do.

Note that because this method depends on synthesis models for the colors of the stellar population, it suffers the same limitations. The model colors depend on the star formation and chemical enrichment history of a given galaxy. At present very simple star formation histories are assumed: either an instantaneous burst or exponentially decaying continuous star formation (which approximates a constant star formation rate for very long decay timescales). These approximations may break down in cases of galaxies which have undergone multiple starbursts separated by long periods, or galaxies which have truncated star formation histories, possibly punctuated by starbursts as well. Dwarf

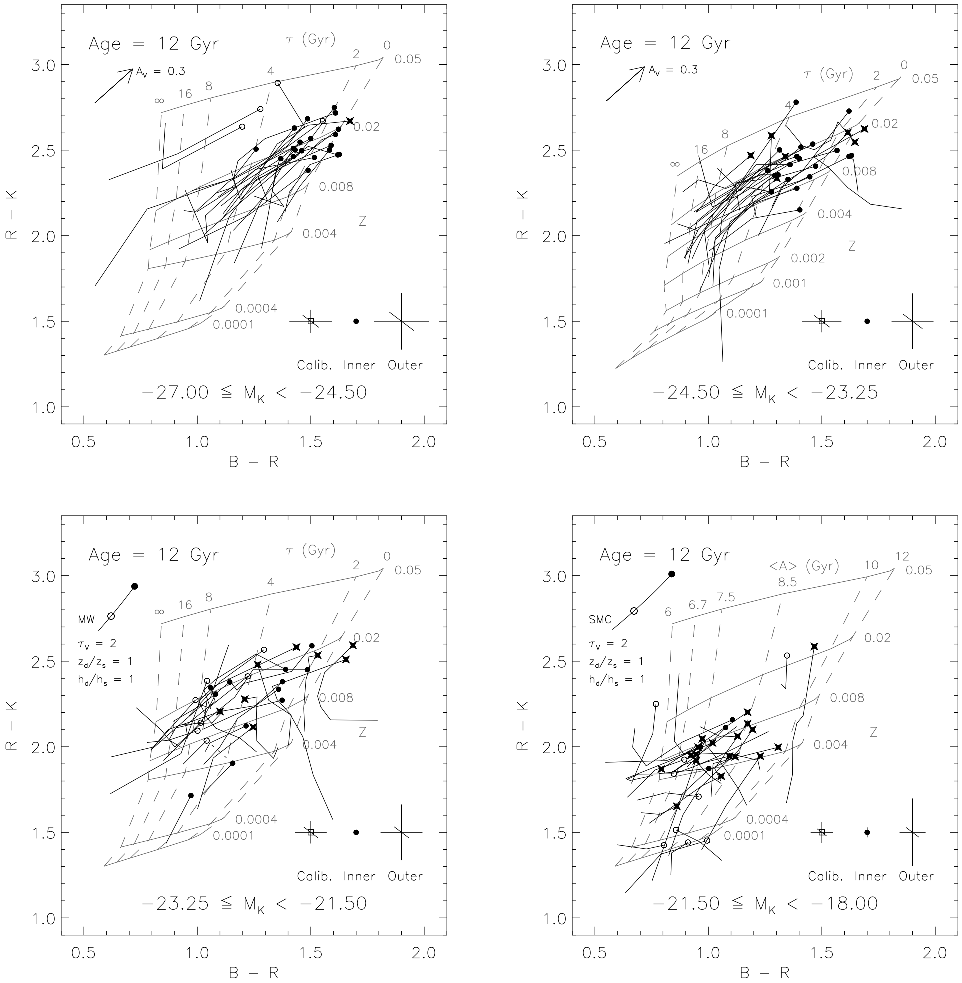

FIGURE 6. Synthetic B–R vs. R–K colors for disk galaxies from Bell & de Jong (2000); see this paper for complete details. Here the four panels show results for galaxies in different ranges of K-band absolute magnitude. The labels on the model grid are the same as in Figure 5; note that the bottom right panel shows the mean age $< A >$ rather than the star formation timescale τ. The solid broken lines in each plot represent observed surface colors for disk galaxies in the Bell & de Jong sample; the attached open or filled circles are the central colors for each galaxy. The symbols in the bottom right of each panel show the calibration and sky subtraction error bars for the inner and outer annuli of a galaxy. Diagram courtesy of Eric Bell.

galaxies, in particular, may not be well-reproduced by the synthesis models. Note also that the sensitivity of the color-color diagram decreases rapidly for very metal-poor or very old stellar populations.

Note also that the mean ages and metallicities of a given position are very sensitive to the dust correction, although the slopes of age and metallicity gradients are not. Finally, the uncertainties in photometry and sky subtraction grow as the surface brightness decreases, so inferred ages and metallicities become increasingly more uncertain in the outer parts of disks and in low surface brightness galaxies. In contrast, metallicity gradients derived from H II regions are more stable, as the luminosity of an H II region is largely independent of its position within a galaxy.

3. Abundances in Local Group Dwarf Elliptical Galaxies

Outside of the Magellanic Clouds, dwarf elliptical galaxies (dEs, sometimes also called dwarf spheroidals, or dSph) are the nearest companion galaxies to the Milky Way. The discovery of the tidally distorted Sagittarius dwarf elliptical (Ibata et al. 1994) brought the number of known dE companions for the Milky Way to nine. There may be more still hidden behind the Galaxy's obscuring dust layer. Recent studies have uncovered a host of dE companions of our sister galaxy M31 as well, and a few other more distant 'free-floating' dEs, such as the Cetus galaxy (Whiting et al. 1999) have been found on Schmidt survey plates. Many of the properties of the Local Group dEs have been tabulated by Mateo (1998).

The dEs are deceptively simple stellar systems, with no young stars and apparently kinematically-relaxed stellar populations. Recent high-precision ground-based and HST CCD photometry have demonstrated that this is far from the truth. The dEs display a variety of complex multi-episode star formation histories. For example, Carina shows evidence for several distinct star formation events spread over several Gyr (Smecker-Hane et al. 1994); Sculptor and Fornax appear morphologically similar, but Sculptor appears to formed the bulk of its stars at an earlier time than Fornax (Tolstoy et al. 2001). Only Ursa Minor appears to have something like a simple, monometallic stellar populations based on its color-magnitude diagram (Mighell & Burke 1999, but see below).

These star formation histories are of vital interest to understanding the evolution of the dEs, and they have raised some puzzles. Among these are the question of how, on the one hand, the dEs lost their gas, and how, on the other hand, they retained gas to experience multiple episodes of star formation! Combining the star formation history with the element enrichment history can, in principle, yield the information needed to understand the evolution of dwarf galaxies and their contribution to enrichment of the IGM.

3.1. *Metallicities*

In the absence of spectroscopy, metallicities for dEs have been derived from their CMDs by comparing the colors of the red giant branches (RGB) with those of globular clusters. This is not entirely satisfactory because of the age-metallicity degeneracy in RGB colors, and because element abundance *ratios*, which also affect RGB colors, may not be the same in the dEs as in the globulars. A few efforts have been able to estimate metallicities from low-resolution spectra obtained with 4-5 meter telescopes; these studies are summarized in Mateo (1998). The photometric and spectroscopic studies show the dEs to have quite low $<$[Fe/H]$>$, ranging from about −1.3 in Fornax to about −2.2 in Ursa Minor. Most of the dEs show evidence for a significant spread in [Fe/H], σ([Fe/H]) = 0.2-0.5 dex, based on the width in color of the RGB (disregarding possible age spread contributing to this).

With several 8-10 meter telescopes now available, medium-resolution (R $\approx$ 5,000) spectroscopy of RGs in the Milky Way satellite dEs can be almost routinely done, while high-resolution spectroscopy (R $>$ 15,000) is possible for the brightest giants. These facilities offer exciting new possibilities for understanding the evolution of the Local Group dEs. One example of what can be done is the VLT study of Tolstoy et al. (2001), who obtained Ca II triplet measurements for 37 red giants in Sculptor, 32 RGs in Fornax, and 23 RGs in the dI NGC 6822. Having measured metallicities for individual stars and

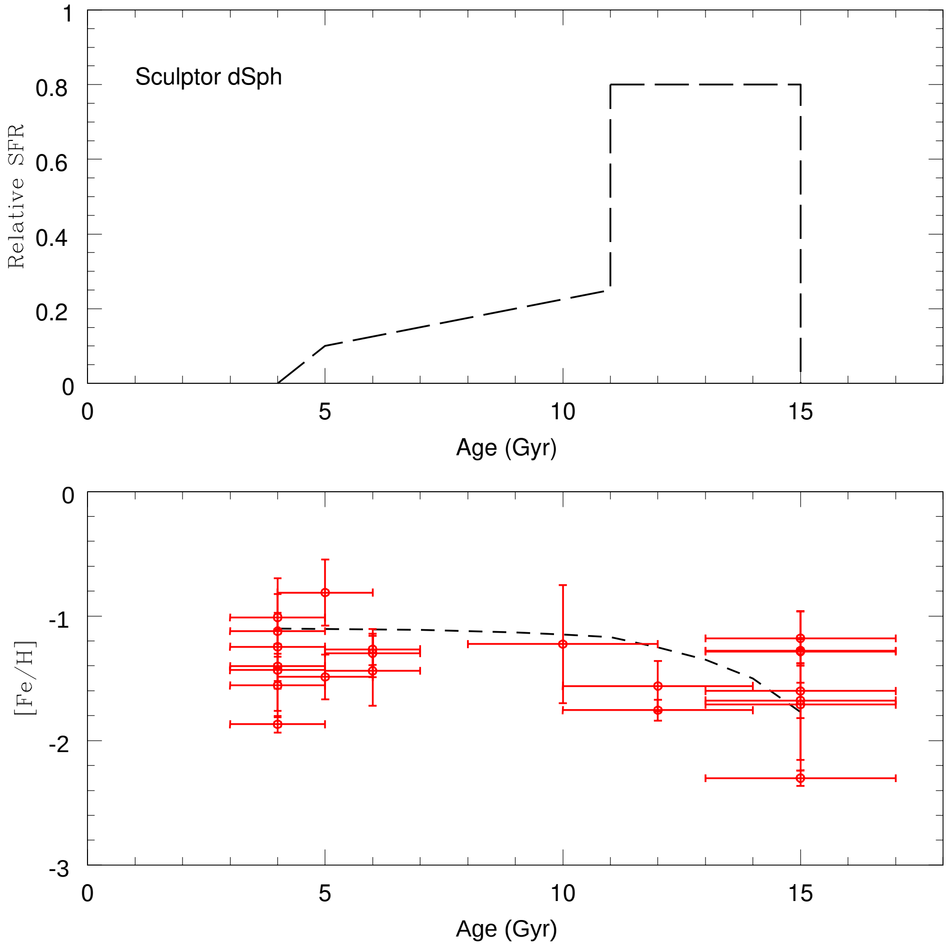

FIGURE 7. The star-formation and metallicity evolution history for Sculptor derived by Tolstoy et al. (2001) from Ca II triplet measurements and photometry of red giants. The upper panel shows a schematic plot of how the star formation rate may have varied over time. The lower panel shows the corresponding variation in metallicity over the same time period (*dashed line*). Overploted on the lower panel are the Ca II triplet measurements for individual Sculptor giants, with ages determined using isochrones.

existing CMDs for these galaxies, it was possible for Tolstoy et al. to assign ages to each star directly by comparison with isochrones of the proper metallicity, and subsequently to derive the time evolution of both the star formation rate and the metallicity. This is shown for Sculptor in Figure 7 taken from Tolstoy et al. The results are consistent with an initial burst of star formation between 11 and 15 Gyr ago with a metallicity [Fe/H] $\approx$ -1.8, a sharp subsequent decline in the SFR, followed by a slow decline in star formation until it stops approximately 5 Gyr ago. The metallicity evolution is very modest, with the youngest stars having a mean [Fe/H] of only -1.4. Their data for Fornax, on the other hand, show a low star formation rate over the time period 10-15 Gyr ago, then a sharply increased rate over the next few Gyr, and a higher mean [Fe/H] of -0.7 for the youngest stars.

The main source of uncertainty here is that the Ca/Fe ratio in these stars may not reflect that of the calibrator globular clusters stars - and the Ca/Fe ratio may actually vary with time within each galaxy! Nevertheless, with more data like this for the Local Group dwarfs it should be possible to derive very accurate evolution histories for these galaxies.

3.2. *Element Ratios*

Element abundance ratios are another important piece of information, since the various elements are synthesized in stars with different masses and lifetimes. The α-element/Fe ratio, in particular is a good diagnostic, because the α-capture elements are produced mainly in very massive stars and expelled into the ISM by Type II or Ib,c supernovae, while Fe is mainly produced in Type I supernovae by longer-lived stars. Thus the α/Fe ratio is an indicator of how rapidly star formation and metal enrichment occurred within a system: high α/Fe indicates enrichment over short time scales, possibly in starburst events, while low α/Fe may indicate enrichment over much longer time scales, as in systems with roughly constant star formation rate over their lifetimes.

Of current interest is the question of whether the Galactic halo was formed in a monolithic collapse (Eggen, Lynden-Bell & Sandage 1962) or was aggregated from mergers of smaller sub-units (Searle & Zinn 1978). It is speculated that the nearby dE satellites may be representative of those sub-units.

It is clear from their CMDs that many of the Milky Way satellites are not like the halo population, since they contain stars that are much young than those in the halo. At the same time, we know that the Sagittarius dE is being tidally disintegrated by the Galaxy and will become part of the halo. Although systems like Fornax and Carina appear not to be representative of the current halo populations, much less complex systems like Ursa Minor and Draco could be similar to the structures out of which the halo formed.

The test of this possibility is that the ages and compositions of stars in the dEs are similar to those in the halo. It is known that halo stars show elevated [α/Fe] compared to disk stars, reflecting a dominant nucleosynthesis contribution from massive stars, while [Ba/Eu] is low in halo stars, indicating that the *s*-process (which is the main source of Ba) has not had sufficient time to contribute to the abundances in halo stars, while the *r*-process (the main source of Eu) dominates in metal-poor stars. Indeed, very metal-poor halo giants show evidence for a purely *r*-process contribution to the abundances of heavy neutron capture elements (Sneden et al. 2000).

Little high-resolution spectroscopy of giants in even the nearest dEs have been carried out because of the faintness of the stars (16th-20th magnitude). However, the first such studies have become available due to the availability of the 10-m Keck telescopes (Shetrone, Coté, & Sargent 2001). Shetrone et al. have obtained high-resolution spectra for 5-6 stars in each of the Draco, Ursa Minor, and Sextans galaxies, deriving abundances for a variety of elements. The comparison of element abundance ratios in these stars show a puzzling mixed bag of results. Although Shetrone et al. argue that [α/Fe] is low in the dEs compared to halo stars, closer examination shows that [Ca/Fe] and [Ti/Fe] do appear to be lower, but [Mg/Fe] and [Si/Fe] appear to agree with halo ratios. Meanwhile, [Ba/Eu] values in the dEs appear to be in good agreement with those in halo stars. The comparison between dEs and halo stars seems to be inconclusive at the present time, perhaps not surprising given the small samples of stars at present. The samples of stars for each galaxy certainly need to be enlarged to determine the evolution of element ratios in these galaxies. Nevertheless, the Shetrone et al. (2001) study illustrates the power of high-resolution spectroscopy with the new large telescopes. More work of this nature is highly encouraged.

4. Abundance Profiles in Spirals and Irregulars

Here I present an overview of the patterns of metallicity and element abundance ratios observed in spiral and irregular galaxies. I will discuss the results for both types of galaxies rather than separately; many aspects can be discussed for the combined groups, although there are a number of differences that could constitute the topic of an entire conference alone.

The observational data to be discussed represent a highly selected sample of abundances, gas masses, and stellar photometry from sources too numerous to mention here. (If you recognize your data in the following plots, feel free to take credit.) I will employ abundances derived almost exclusively from H II region spectra, since they contribute the largest set of abundance data for spirals and irregulars in the local universe.

4.1. *Gas and Stellar Masses*

The ultimate goal of any chemical evolution model is to account for the global and local metallicity within a galaxy, the gas and stellar mass distributions, and the stellar luminosity self-consistently. Thus, any discussion of abundances and chemical evolution should include a few words about observational determinations of gas and stellar masses and mass surface densities.

4.1.1. *Neutral and Molecular Gas*

Neutral gas is the largest component of gas in most spirals and irregulars, as determined from H I 21-cm hyperfine line measurements. The 21-cm line has been well-mapped in many nearby galaxies. With regard to determining gas fractions and surface densities, a few points should be kept in mind:

(*a*) *The size of the neutral gas disk is often much larger than the stellar disk in spirals and irregulars*, as much as 3-4 times the photometric radius R_{25} (e.g., Broeils & van Woerden 1994). One must obtain or use maps which cover the full extent of the H I disk, which can mean observing over degree-size scales for the nearest spirals. Determining the H I extent may be difficult in complicated interacting systems such as the M81 group (Yun et al. 1994).

(*b*) *Fully sampled maps are desirable.* Aperture synthesis maps, while providing the high spatial resolution needed for studies of kinematics and gas structure, can miss a large fraction of the H I emission on scales larger than the synthesized beam due to lack of short antenna baselines in the $u - v$ plane. (The closest spacings in an interferometer are, of course, one antenna diameter.) This is especially true for the highest resolution images. Although there are efforts to correct for the missing extended emission by including single-dish measurements, it is usually assumed that the extended emission is uniformly distributed. This assumption may not be correct.

(*c*) *The helium contribution to the mass is not negligible.* The helium accounts for 30-40% of the total gas mass, which must be included in the total gas mass and surface density.

Fortunately, many nearby galaxies have been well mapped in H I at kiloparsec scale resolution or better.

Molecular gas, mostly in the form H_2, is the important phase associated with star formation. Although H_2 may not dominate the total gas mass, it is often found to be the main component in the inner disk of Sbc or later type spirals, and so can be the main contribution to the gas surface density in such regions.

H_2 has no dipole moment and thus emits no strong dipole radiation of its own. The usual tracer of molecular gas is the abundant CO molecule, typically the ^{12}CO (J=1–0) millimeter-wave transition. The conversion from the measured I(CO) to the column density $N(H_2)$, X(CO), must be calibrated largely without the benefits of direct measurement of H_2 column densities. The result has been a long-standing controversy over the value of the CO-H_2 conversion factor and its dependence on metallicity. For example, Wilson (1995) has studied the CO-$N(H_2)$ relation in a variety of environments in Local Group galaxies, comparing $I(CO)$ with molecular cloud masses derived from the velocity dispersion assuming the clouds are in virial equilibrium. From her data Wilson found a roughly linear relation between X(CO) and 12 + log O/H corresponding to approximately a factor ten increase in X(CO) for factor ten decrease in O/H, from solar O/H to 0.1 times solar O/H. On the other hand, Israel (1997a,b) argues that virial equilibrium is a poor assumption for short-lived molecular clouds. He instead uses the FIR dust emission surface brightness and H I maps to determine the dust/N(H) ratio, then uses the FIR surface brightness to estimate $N(H_2)$ in regions where CO is detected. With this method Israel derives a variation in X(CO) with O/H which is much steeper than that obtained by Wilson: a factor of approximately 100 decrease in X for a factor 10 increase in O/H.

Both of these methods likely suffer from errors due to assumptions made. Virial equilibrium may very well be a poor assumption for molecular clouds. On the other hand, the FIR calibration depends on the assumption that the dust-to-gas ratio is the same in neutral gas and in molecular clouds; however, grains may be preferentially destroyed by shocks in the lower density neutral component. The FIR model is also very sensitive to the dust temperature. The relation between I(CO) and $N(H_2)$ likely depends on a variety of factors besides metallicity (Maloney & Black 1988). More work needs to be done to determine the best method to obtain H_2 masses.

4.1.2. *Stellar Mass Densities*

Masses and surface densities for the stellar component in galaxies are probably even more uncertain than molecular gas masses. Because of the flat rotation curves of disk galaxies, and the consequent inference that the galaxies are dominated by non-luminous, non-baryonic matter, the mass-to-light (M/L) ratio and mass surface density of the stellar component can not be derived from galaxy dynamics. Unless one can count the stars in a region directly (possible only for very nearby systems), it is necessary to infer M/L for the stellar component by indirect means. This is difficult because the luminosity and colors of composite stellar populations depend on both the star formation history and the metal enrichment history.

Nevertheless, recent work by Bell & de Jong (2001) indicates that the stellar M/L ratios of galaxies are rather robustly related to their colors. Bell & de Jong examined population synthesis models for galaxies assuming a variety of star formation histories. They found that M/L for the stellar component correlated very well with optical colors, although there is some scatter in the correlations. IR colors did not correlate as well with M/L because of the strong metallicity dependence of the IR luminosity of giants. The B-band M/L ratio shows a steep correlation with color, while the K-band M/L ratio shows a much less steep correlation (a factor three increase between B–R = 0.6 and B–R = 1.6, compared to a factor 10 increase in B-band M/L over the same color range). If the population synthesis models can reliably reproduce the colors and spectra of real galaxies, this method offers the possibility of greatly improved estimates of masses and mass surface densities for the stellar components of disk galaxies.

4.2. *Spatial Abundance Profiles*

The spatial distribution of abundances in galaxies depends coarsely on the Hubble type. Spectroscopic study of H II regions in unbarred or weakly barred spiral galaxies typi-

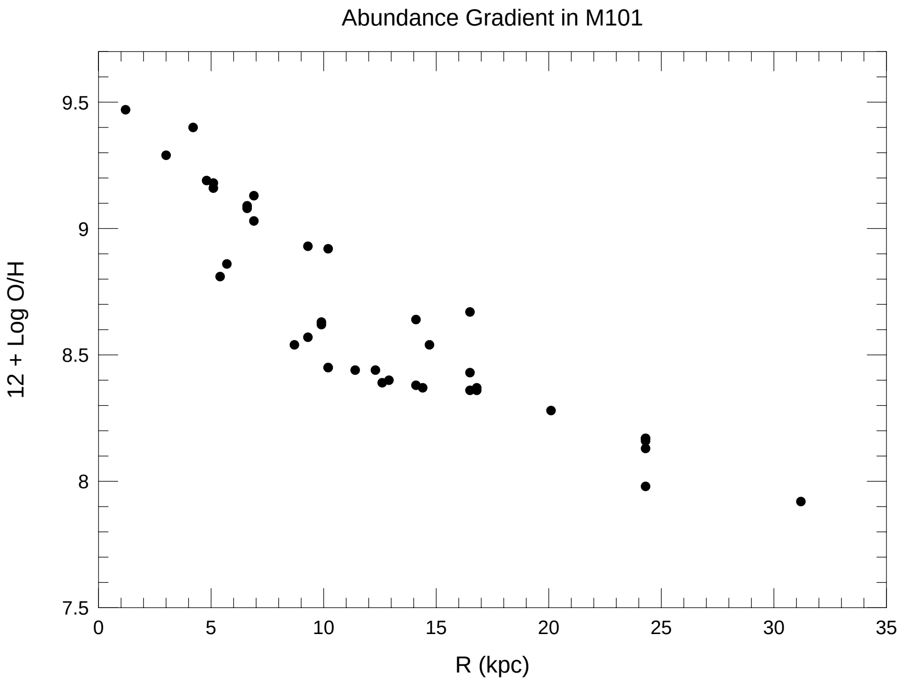

FIGURE 8. The gradient in O/H across the disk of the spiral galaxy M101 vs. galactocentric radius (Kennicutt & Garnett 1996).

cally reveals a strong radial gradient in metallicity (Figure 8), as determined from O/H (Zaritsky, Kennicutt, & Huchra (1994; ZKH); Vila-Costas & Edmunds 1992; VCE). The derived O/H can drop by a factor of ten to thirty or fifty from the nucleus of a galaxy to the outer disk as demonstrated in galaxies with well-sampled data. In those spirals with spectroscopy of more than ten H II regions covering the full radial extent of the disk, there is little evidence that O/H gradients deviate from exponential profiles. Irregular galaxies, by contrast, show little spatial variation in abundances, to high levels of precision (Kobulnicky & Skillman 1996), indicating a well-mixed ISM. The data for strongly barred spiral galaxies shows evidence that their O/H gradients are more shallow than in unbarred spirals. I will discuss these galaxies in more detailed in a later section.

A quick glance at data on O/H in galaxies (e.g. Figure 8 of ZKH) does not immediately reveal any trends of metallicity among galaxies of different types. However, detailed examination of this data shows that there are significant correlations between abundances and abundance gradients in spirals and irregulars with galaxy structural properties. Here I shall review some of these correlations and some implications. Note also that for the most part this discussion applies only to high surface brightness "normal" spirals.

4.3. *Metallicity versus Galaxy Luminosity/Mass*

One well established correlation is the relation between metallicity and galaxy luminosity or (Garnett & Shields 1987, Lequeux et al. 1979). This is shown in the top panel of Figure 9, where I plot O/H determined at the half-light radius of the disc (R_{eff}) versus B-band magnitude M_B. This is the usual way of plotting the relation. [Note that the

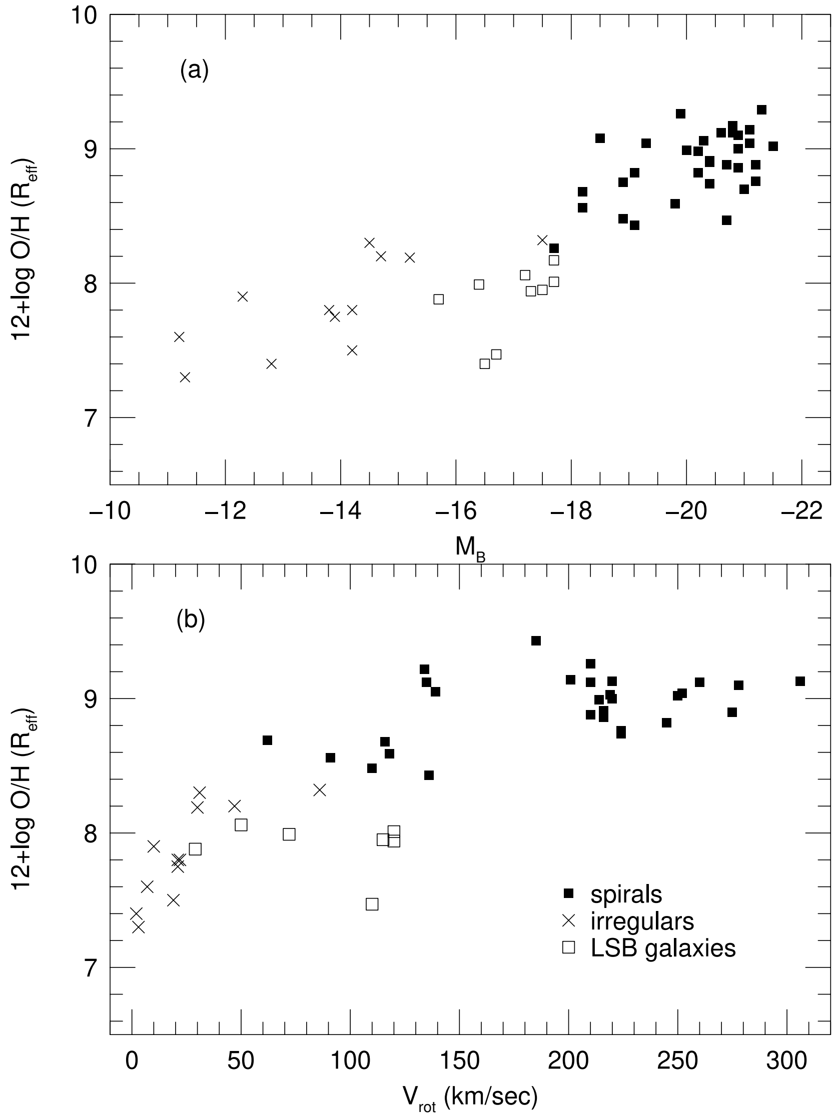

FIGURE 9. Top: The correlation of spiral galaxy abundance (O/H) at the half-light radius of disk from the galaxy nucleus vs. galaxy blue luminosity. Bottom: abundance versus maximum rotational speed V_{rot}.

choice of what value of metallicity to use for spiral disks, where the metallicity is not constant, is somewhat arbitrary. I have used the value at one disk scale length in the past on the grounds that the disk scale length is a structural parameter determined by galaxy physics, whereas the photometric radius can be biased by observational considerations.

The actual "mean" abundance in the disk ISM would be determined by convolving the abundance gradient with the gas distribution. As a simple compromise I have used the disk half-light radius, which is 1.685 times the disk scale length (de Vaucoleurs & Pence 1978), and so is still connected to galaxy structure. It should be noted also that a O/H - M_B correlation is derived whether one uses the central abundance, the abundance at one disk scale length, or some other fractional radius.] ZKH noted the remarkable uniformity of this correlation over 11 magnitudes in galaxy luminosity, for ellipticals and star-forming spiral and irregular galaxies.

To the extent that blue luminosity reflects the mass of a system, the metallicity-luminosity correlation suggests a common mechanism regulating the global metallicity of galaxies. What the mechanism might be is not very well understood at present. The most commonly invoked mechanism is selective loss of heavy elements in galactic winds (e.g., Dekel & Silk 1986). However, the metallicity-luminosity correlation for star-forming galaxies by itself does not imply that lower-luminosity galaxies are losing metals. Such a correlation could occur if there is a systematic variation in gas fraction across the luminosity sequence, either because the bigger galaxies have evolved more rapidly, or because the smaller galaxies are younger. In fact, there is evidence that both of these may be true. There is also evidence for fast outflows of hot X-ray gas from starburst galaxies such as M82 (Bregman, Schulman, & Tomisaka 1995). However, the question of whether this hot gas is escaping into the IGM or will be retained by any given galaxy depends not just on the gravitational potential, but also on details such as the vertical distribution of ambient gas and the radiative cooling which are not so well understood.

The question of loss of metals from galaxies is profound because of the existence of metals in low column density Lyman-α forest systems (Ellison et al. 1999), which are probably gas clouds residing outside of galaxies. Where the heavy elements came from in these systems is still a mystery; it is possible that they were seeded with elements from a generation of pre-galactic stars or with elements expelled in starbursts during galaxy formation. In the dense environments of galaxy clusters, ram pressure stripping by intracluster gas, tidal interactions, and galaxy mergers may also liberate material to the intracluster medium (Mihos 2001). It is therefore a useful exercise to investigate what kinds of galaxies are potential candidates for ejecting heavy elements into the IGM.

I begin by looking at the metallicity-luminosity relation in a different way. It is often argued that the B-band luminosity is not a very good surrogate for mass, since the B-band light can be affected by recent star formation and dust. Therefore, in Figure 9(b) I plot the mean O/H for the galaxies in Fig. 9(a) versus rotation speed (obtained from resolved velocity maps [e.g., Casertano & van Gorkum 1991, Broeils 1992], not single-dish line widths), where for the spirals the rotation speed is taken to be the value on the flat part of the rotation curve. Interestingly, the Z-V_{rot} correlation turns over and flattens out for $V_{rot} \gtrsim 150$ km s-1, suggesting that spirals with rotation speeds higher than this have essentially the same average metallicity. Does this indicate a transition from galaxies that are likely to be losing metals to the IGM to galaxies that essentially retain the metals they produce?

This question can be examined further by studying metallicity as a function of gas fraction. In the context of the simple, closed box, chemical evolution, Edmunds (1990) derived a few simple theorems that show that outflows of gas and inflows of metal-poor gas cause galactic systems to deviate from the closed box model in similar ways. Specifically, defining the effective yield y_{eff}

$$y_{eff} = \frac{Z}{ln(\mu^{-1})}, \tag{4.6}$$

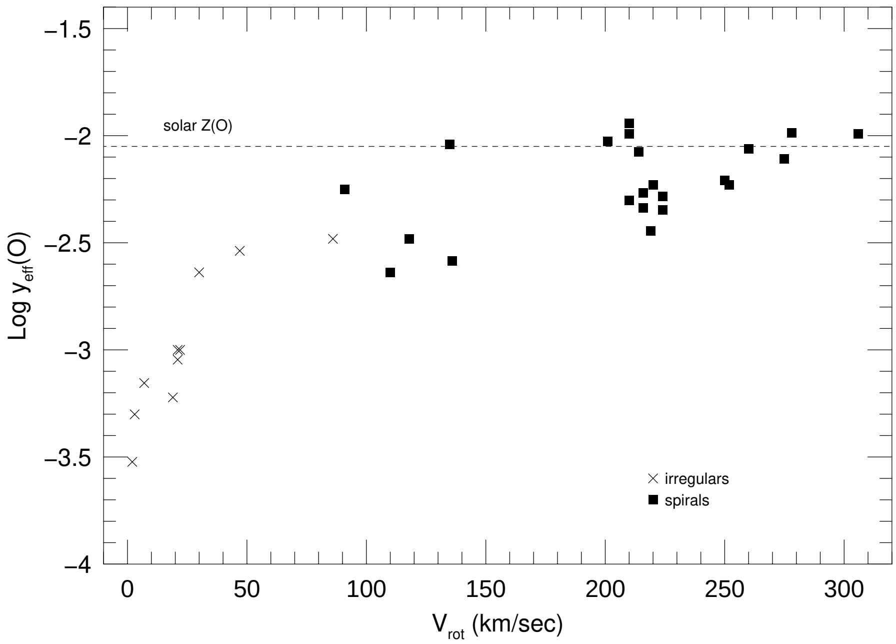

FIGURE 10. Effective yields y_{eff} for nearby spiral and irregular galaxies versus rotation speed V_{rot} (Garnett 2002). Filled squares represent the data for spirals while the crosses show the data for irregulars.

outflows of any kind and inflows of metal-poor gas tend to make the effective yield smaller than the true yield of the closed box model. y_{eff} defined this way is an observable quantity, and provides a tool for studying gas flows in galaxies. Although the true yield is relatively uncertain, comparing effective yields for a sample of galaxies can provide information on the relative importance of gas flows from one galaxy to another.

Such a comparison is presented in Figure 10 (Garnett 2002), where I show data compiled on abundances, atomic and molecular gas, and photometry for 22 spiral and 10 nearby irregular galaxies. Figure 10 plots the effective yields derived for each galaxy using equation 3.1 and the global gas mass fraction versus galaxy rotation speed. The plot shows a very strong systematic variation in y_{eff} with V_{rot} in the dwarf irregular galaxies, with y_{eff} increasing asymptotically to a roughly constant value for the most massive galaxies. The uncertainties in the individual y_{eff} values are relatively large, because of relatively large uncertainties in M/L ratios for the stellar component and the CO - H_2 conversion for the molecular gas component; individual values of y_{eff} are probably not known to better than a factor of two. Nevertheless, the data show a factor of 30 systematic increase in y_{eff} from the least massive irregulars to the most massive spirals.

This result is striking verification that the yields derived for dwarf irregulars are significantly lower than in spiral galaxies, and shows that the variation is a systematic function of the galaxy potential. In strict terms, the trend in Figure 10 does not distinguish between infall of unenriched gas and outflows as the cause. However, the trend toward small y_{eff} in the least massive galaxies suggests that it is the loss of metals in galactic winds that drives the correlation. It would be of interest to use this correlation to estimate the total amount of gas lost in the small systems, and to determine the manner in which supernova energy feeds back into the ISM of the host galaxies.

Although not quite certain yet where one can say that galaxies are losing significant quantities of metals and which ones retain essentially all their metals, it appears likely that this boundary point is somewhere near $V_{rot} \approx 150$ km s^{-1}. Given this, one can surmise that the outflow of hot gas seen in the starburst galaxy M82 ($V_{rot} \approx 100$ km s^{-1}) may contribute significantly to enrichment of the IGM, while the hot gas flow seen in NGC 253 ($V_{rot} \approx 210$ km s^{-1}) is likely to remain confined to the galaxy.

4.4. *Abundance Gradient Variations*

Another commonly-noted correlation is illustrated in the top panel of Figure 11: the steepness of abundance gradients (expressed in dex/kpc) decreases with galaxy luminosity. However, more luminous galaxies have larger disk scale lengths, and so if one looks at the gradient per disk scale length (Figure 11, bottom panel), the correlation goes away. Interestingly, when one considers the errors in the computed gradients (25% is a typical uncertainty), then the scatter in measured gradient slopes may be consistent with purely observational scatter. Combes (1998) has suggested that a "universal" gradient slope per unit disk scale length may be explained by so-called "viscous disk" models (Lin & Pringle 1987); if the timescale for viscous transport of angular momentum is comparable to the star formation timescale (with the two timescales connected through the gravitational instability perhaps), such models naturally produce an exponential stellar disk. Chemical evolution models invoking viscous transfer have been able to produce abundance gradients (Clarke 1989; Tsujimoto et al. 1995), but it is not yet clear from the few models examined that they can yield very similar abundance gradients per unit disk scale length for a wide variety of spiral disks. This is something that deserves further study.

Another interesting possibility is presented by Prantzos & Boissier (2000). They constructed a sequence of chemical evolution models for disk galaxies by scaling the mass distribution (total mass, scale length) according to the scaling relations for cold dark matter halos of Mo, Mao & White (1998), in which the disk mass profile can be expressed using only two parameters: the maximum circular velocity (which corresponds to the halo mass) and the spin parameter λ (which corresponds to the angular momentum). A key assumption is that the scaled galaxies settle into exponential disks. Prantzos & Boissier computed models for galaxies under these assumptions, calibrated by reproducing measurements for the Milky Way. The basic results are illustrated in their Figure 4, reproduced here in Figure 12. The top panel plots the slope of the composition gradients in units of physical length (kiloparsecs) vs. M_B, the middle panel plots the gradients per unit disk scale length, while the bottom panel plots the gradient over the photometric radius R_{25}. In each case the model gradients are in good agreement on average with observed gradients, although the gradients per unit scale length and R_{25} are perhaps a bit steeper than observed. If this analysis holds up it would be quite remarkable, as it would have been difficult to imagine that the present-day ISM composition could be related to the initial properties of the disks in the distant past. This may reflect the assumption that the baryons start out with exponential mass distributions. Prantzos & Boissier (2000) predict that there should be a small spread in observed gradients per kiloparsec in massive spirals and a large spread in small spirals, such that small spirals with large angular momentum should have shallower gradients (larger scale lengths) than those with lower angular momentum.

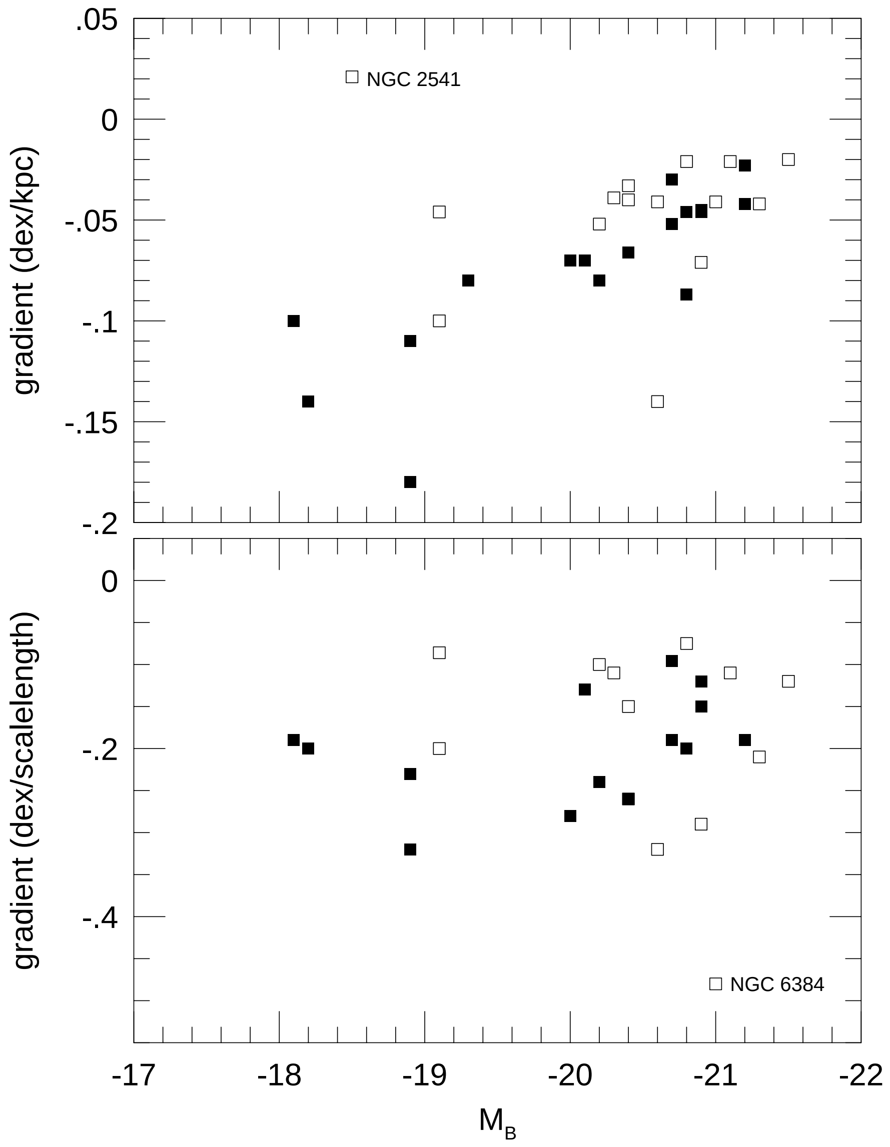

FIGURE 11. The correlation of abundance gradient vs. M_B, from Garnett et al. (1997a). The upper panel shows abundance gradients per kpc, while the lower panel shows gradients per unit disk scale length.

4.5. *Metallicity vs. Surface Brightness*

The uniformity of abundance gradients as a function of scale length suggests a close correlation between metallicity and disk surface brightness. Indeed, McCall (1982) and Edmunds & Pagel (1984) noted a remarkably tight correlation between O/H and disk

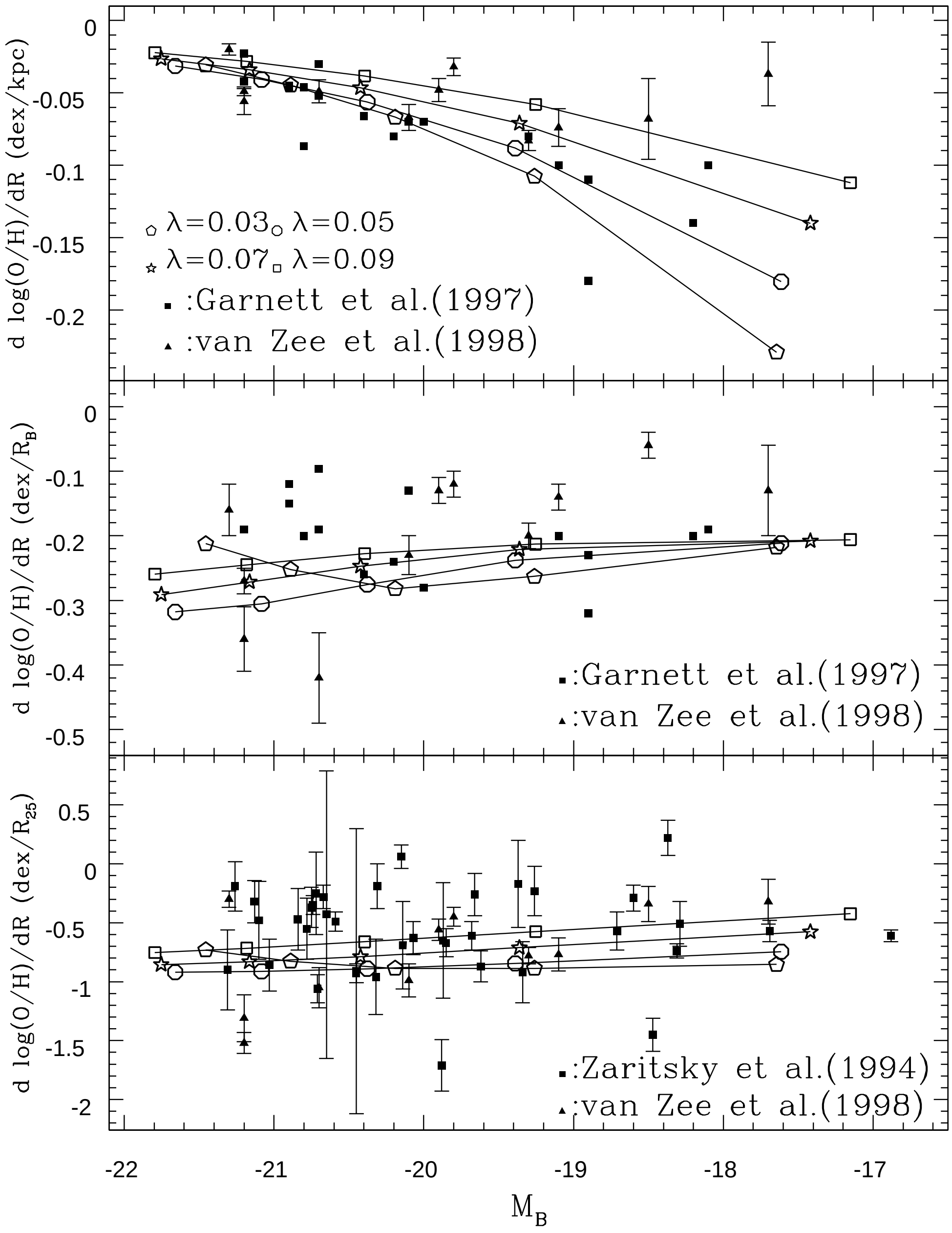

FIGURE 12. Comparison of generalized chemical evolution models from Prantzos & Boissier (2000) with observed composition gradients for spiral galaxies. Top: O/H gradient in dex/kpc vs. M_B. Middle: O/H gradient in dex per unit disk scale length vs. M_B. Bottom: O/H gradient over the photometric radius R_{25} vs. M_B. The curves show the model relations for constant λ for $\lambda = 0.03$, 0.05, 0.07, and 0.09.

surface brightness for late-type spirals. This has provided part of the motivation for

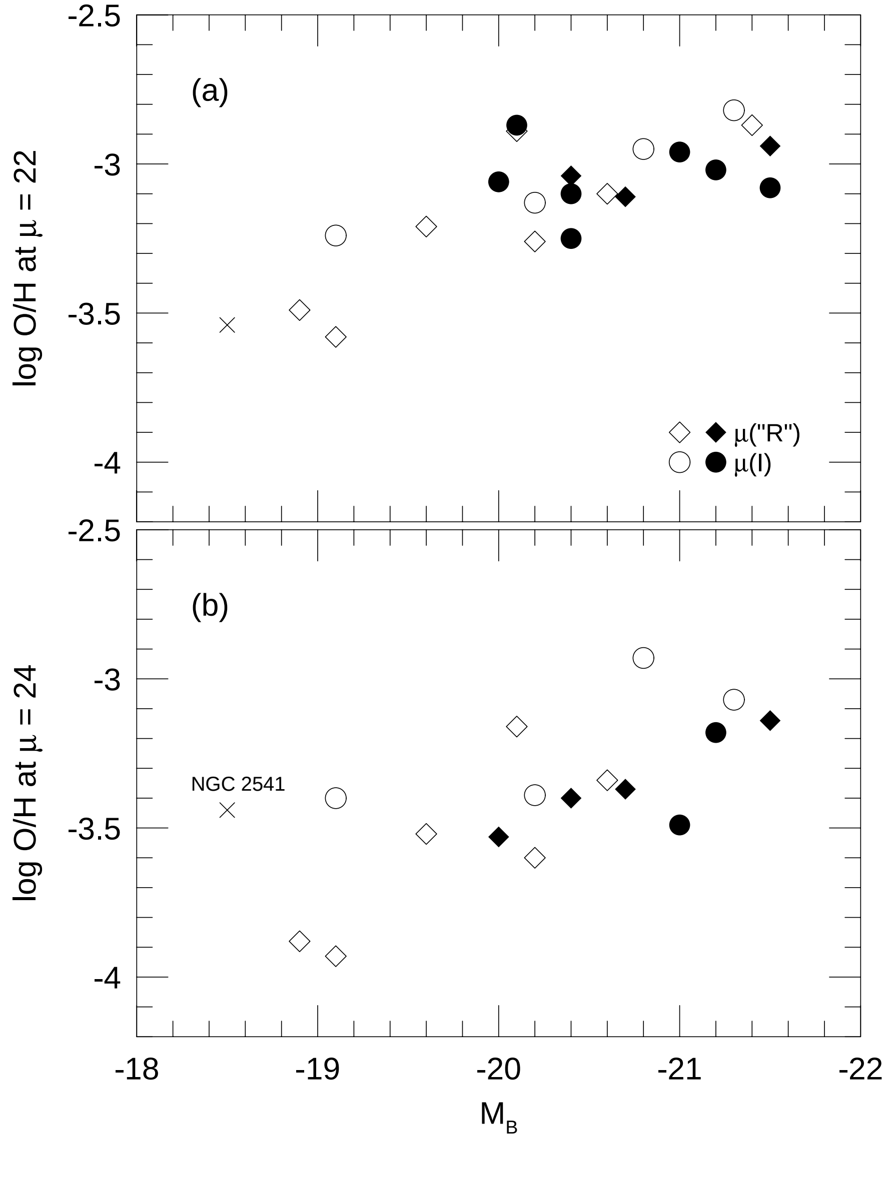

FIGURE 13. O/H at fixed value of galaxy surface brightness vs. M_B. Top: abundances at 22 mags arcsec^{-2}. Bottom: abundances at 24 mag arcsec^{-2}. More luminous spirals have higher abundances at a fixed surface brightness. Open symbols are from Garnett et al. (1997a); filled symbols represent additional data obtained from the literature.

models of self-regulated star formation, in which the radiation and mechanical energy produced by stars feeds back into the surrounding ISM and acts to inhibit further star formation. Models of this kind have been explored by Phillips & Edmunds (1991) and

Ryder (1995), and appear to do a good job of reproducing the trends of both star formation rate and O/H with surface brightness. One caveat is that the interaction of the stellar energy output with the ISM is still poorly understood. Viscous disk models also provide a possible mechanism to tie the abundances to the underlying surface density distribution.

Edmunds & Pagel (1984) also noted that early-type spirals do not follow the same O/H-surface brightness correlation as the late types. Garnett et al. (1997a) put this on a more quantitative basis. Figure 13 displays the characteristic metallicity at two fixed values of disk surface brightness for a sample of spirals having either I- or R-band surface photometry; these bandpasses presumably sample the light from the old disk population better than B. The figure shows that metallicity-luminosity correlation appears to hold at all values of surface brightness across spiral disks. This result argues for two modes of enrichment in disk galaxies: a local mode, in which the metallicity is connected to the local mass density, and a global mode, in which an entire galaxy is enriched in a manner dependent on its total mass. One can imagine a global enrichment event which raises the metallicity of a galaxy to some level which depends on total mass, followed by sequential local enrichment which follows the mass density distribution. One caveat is that M/L, and thus the mass surface density at a given surface brightness, may vary systematically along the luminosity sequence in Figure 13. A more comprehensive study of mass surface density and gas fraction along this sequence should prove enlightening.

4.6. *Barred Spirals*

Bars are interesting because the gravitational potential of a bar is expected to induce a large-scale radial gas flow, possibly through radiative shocking and subsequent loss of angular momentum as the gas passes through the bar (Barnes 1991). The radial flow could significantly alter the metallicity distribution by mixing in gas from outer radii, thus weakening composition gradients, and is often argued to be the means to fuel the nuclei of active galaxies. The evidence so far accumulated indicates that barred spirals generally do have shallower composition gradients than weakly-/non-barred spirals (ZKH; Martin & Roy 1994). Martin & Roy (1994) have argued that the slope of the composition gradient correlates with both bar length and bar strength, defined as the ratio of bar length to width. This is illustrated in Figure 14, which shows the slope of the O/H gradient per kpc versus bar length a relative to the photometric radius (*top panel*) and versus bar strength $E_B = 10(1-b/a)$, where b is the bar width. Non-barred, barred, and irregular galaxies from the Martin & Roy sample are distinguished by different symbols, and the gradients have been adjusted for new distances to the galaxies. The plots show that (1) the non-barred spirals show a wide range of values for gradient slopes, although on average they are steeper than those for barred spirals; and (2) the O/H gradients for the barred spirals tend to get shallower with increasing bar length and bar strength. On the other hand, the trend depends how the gradients are scaled; if one plots the O/H gradient per unit scale length instead, the correlations disappear.

Curiously, some barred spirals (e.g., NGC 1365; Roy & Walsh 1997) show an O/H gradient within the bar, with flattening only outside the bar. One way to explain this is if strong star formation occurs in the bar, building up abundances faster than the radial flow can homogenize them (Friedli, Benz, & Kennicutt 1994).

4.7. *Spiral Bulges*

Abundances in bulges generally are obtained the same way as for ellipticals, by spectroscopy and modeling of absorption line indices from the integrated stellar population, and so suffer from the same uncertainties. Most of the line indices in the Lick system

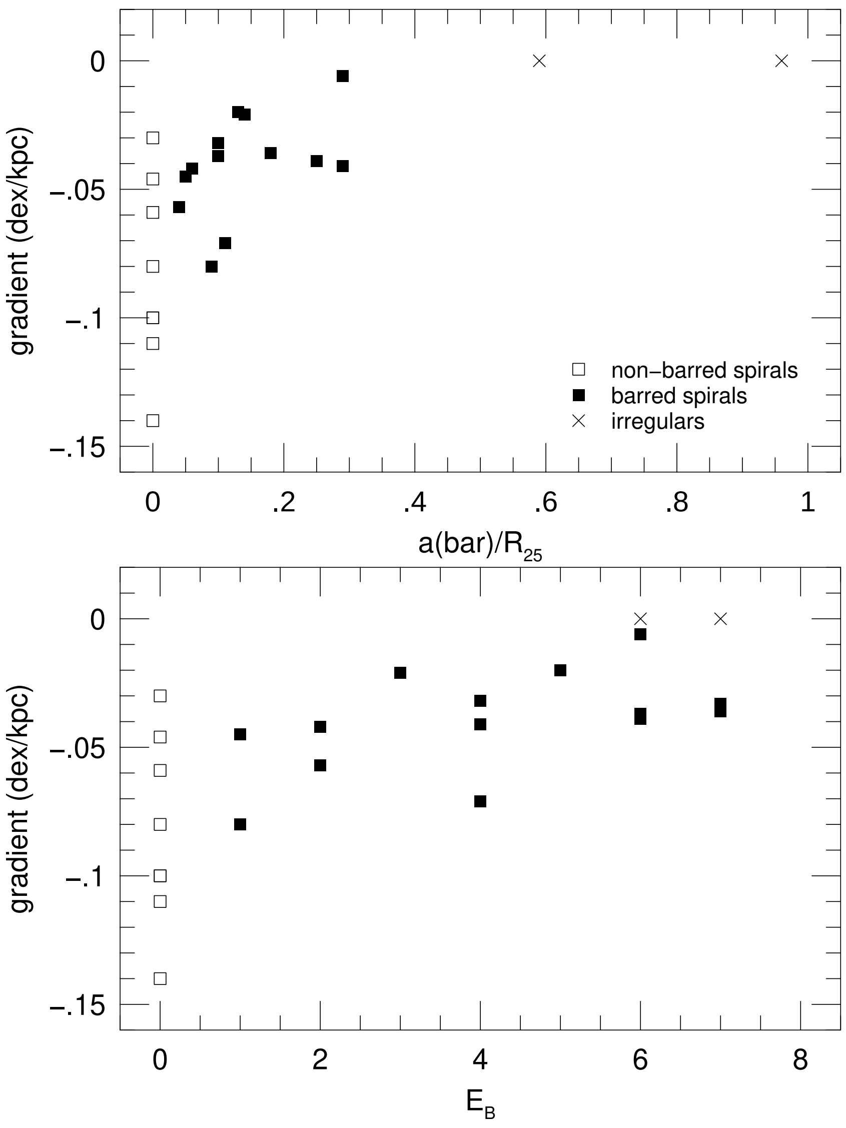

FIGURE 14. *Top:* O/H gradient per kpc vs. bar length a relative to the photometric radius R_{25}. Filled squares are barred spirals, unfilled squares non-barred spirals, and crosses are irregular galaxies. Bottom: O/H gradient vs. bar strength $E_B = 10(1-b/a)$, where b/a is the ratio of bar minor and major axes. Plot adapted from Martin & Roy 1994.

vary in the same way with age and metallicity, and so poorly distinguish between the two in model grids. A few, such as Hβ, Mg b, Fe5270, and Fe5335, do provide some ability to separate age and metallicity, and have been used to obtain estimates of ages, [Fe/H], and [Mg/Fe] in spheroidal systems (Worthey 1998).

Most work on abundances in bulges have come from spectroscopy of the central regions. Jablonka, Martin, & Arimoto (1996) found that Mg_2 correlated with both bulge luminosity and stellar velocity dispersion in spirals with T = 0-5, but that the Fe5270 feature did not. Comparing with a grid of synthetic spectra with non-solar [α/Fe] they inferred that [Mg/Fe] increased with bulge luminosity as well. Similar results are obtained for ellipticals (Worthey 1998). Maps of spectral line indices obtained with integral field units (Peletier et al. 1999, de Zeeuw et al. 2002) show hints that Mg/Fe varies with radius, although only a small number of galaxies have been analyzed so far.

High-resolution spectroscopy of red giants in our own Galactic bulge recommends caution in interpreting line indices in integrated spectra of ellipticals and bulges. Giants in the Baade's Window region show high α/Fe ratios and a mean [Fe/H] ≈ -0.25, similar to [Fe/H] for solar neighborhood stars (McWilliam & Rich 1994). The mean metallicity is lower by about 0.3 dex compared to low-resolution spectroscopic and photometric determinations. This has several implications. Enhanced Ti/Fe ratios make the spectral types of the bulge giants later for the same IR colors compared to stars with solar abundance ratios. Enhanced α/Fe alter both stellar line indices and the location of isochrones in population synthesis models, which have been computed using solar abundance ratios so far. Thus, metallicities derived for spheroids may be overestimated by a factor of two or so. Most population synthesis Trager et al. (2000a,b) attempt to correct the models for the effects of non-solar element abundances ratios. Such corrections are non-trivial, as both isochrones and line strengths are affected. No such corrections have been applied to bulges yet.

The formation of bulges is still mysterious. The candidate mechanisms are: monolithic collapse with rapid star formation (Eggen, Lynden-Bell, & Sandage 1962); mergers of roughly equal mass objects in hierarchical clustering models for galaxy formation (Baugh, Cole, & Frenk 1996: Kauffmann 1996); and secular growth from disk material, for example by mass transfer via bars (Combes et al. 1990; Hasan, Pfenniger, & Norman 1993). High α/Fe (that is, higher than the solar ratio) would tend to favor the models with rapid bulge formation from relatively metal-poor gas, because most of the Fe is expected to come from Type Ia supernovae. Solar or less α/Fe would tend to favor secular evolution from already enriched material, or star formation extended over times cales greater than 1 Gyr. The correlation of Mg/Fe with bulge luminosity and velocity dispersion suggests that a mix of formation mechanisms are at work; moreover, Andredakis et al. (1995) have found that bulge structure parameters correlate with Hubble type and bulge luminosity, such that large, luminous bulges tend toward $R^{1/4}$ profiles similar to ellipticals, while small bulges tend to have exponential profiles (although de Jong 1996 argues that bulges have exponential profiles in general). The trends in Mg/Fe and bulge shape together suggest that large bulges formed rapidly at early times, while small bulges may have formed more slowly via secular processes.

4.8. *Cluster Spirals and Environment*

Environment and interactions appear to play a significant role in the evolution of galaxies, particularly in dense environments. Interactions with satellites may be responsible for the significant fraction of lopsided spiral galaxies (Rudnick & Rix 1998). Disk asymmetry may affect the inferred spatial distribution of metals in the interstellar gas. For example, Kennicutt & Garnett (1996) noted an asymmetry in O/H between the NW and SE sides of M101, which may be related to the asymmetry in the structure of the disk. Zaritsky (1995) found a possible correlation between disk $B-V$ and the slope of the O/H gradient such that bluer galaxies tended to have steeper gradients. He suggested that accretion of metal-poor, gas-rich dwarf galaxies in the outer disk could steepen abundance gradients and make the colors bluer through increased star formation. On the other hand, the trend may simply reflect the fact that spirals with steep metallicity gradients tend to be lower-luminosity late Hubble types with bluer colors on average.

Rich clusters offer a variety of galaxy-galaxy and galaxy-ICM interactions. The cluster environment certainly affects the morphology of galaxies (Dressler 1980). It is also known that spirals near the center of rich clusters, for example, the Virgo cluster, show evidence for stripping of H I, especially from the outer disks (Warmels 1988; Cayatte et al. 1994). Such stripping is inferred to result from interaction of the galaxy ISM with the hot X-ray intracluster gas. The degree of H I stripping correlates with projected distance from the cluster core, although in Virgo the molecular content appears to be not affected (Kenney & Young 1989).

If field galaxies evolve through continuing infall of gas (Gunn & Gott 1972), then the truncation of H I disks in cluster spirals should have an effect on the chemical evolution. Specifically, infall of metal-poor gas reduces the metallicity of the gas at a given gas fraction. Truncation of such infall should then cause the chemical evolution of cluster spirals to behave more like the simple closed box model, and thus should have higher metallicities than comparable field spirals. This idea has led to several studies of oxygen abundances in Virgo spirals. The largest study so far is that of Skillman et al. (1996), who obtained data for nine Virgo spirals covering the full range of H I deficiencies. The results indicate that cluster spirals with the largest H I deficiencies have higher O/H abundances than field spirals with comparable M_B, rotation speeds, and Hubble types, while spirals with only modest or little H I stripping have abundances comparable to those of similar field spirals (Skillman et al. 1996, Henry et al. 1994, 1996). The samples studied so far have been small, and one must worry about possible systematic errors in abundance caused by the lack of measured electron temperatures. This is an area that could benefit from further study with larger galaxy samples and more secure abundance measurements.

5. Element Abundance Ratios in Spiral and Irregular Galaxies

The abundance ratios of heavy elements are sensitive to the initial mass function (IMF), the star formation history, and variations in stellar nucleosynthesis with, e.g., metallicity. In particular, comparison of abundances of elements produced in stars with relatively long lifetimes (such as C, N, Fe, and the s-process elements) with those produced in short-lived stars (such as O) probe the star formation history. Below, I review the accumulated data on C, N, S, and Ar abundances (relative to O) in spiral and irregular galaxies, covering two orders of magnitude in metallicity (as measured by O/H). The data are taken from a variety of sources on abundances for H II regions in the literature.

5.1. *Helium*

Helium, the second most abundant element, has significance for cosmology and stellar structure. Most ^{4}He was produced in the Big Bang, and the primordial mass fraction Y_p is a constraint on the photon/baryon ratio and thus on the cosmological model. The He mass fraction also affects stellar structure, but He is difficult to measure in stars and so must be inferred from other measurements. On the other hand, He I recombination lines are relatively easy to measure in H II regions, and so a large amount of data is available on He/H in ionized nebulae.

A great deal of effort has been spent in determining Y_p, and is covered in Gary

Steigman's contribution, so I will be brief on this aspect. Peimbert & Torres-Peimbert (1974) initiated the current modern study of Y_p by making the simple assumption that the He mass fraction varies linearly with metallicity (or O/H), and thus used measurements of abundances in H II regions with a range of O/H to extrapolate to the pre-galactic He abundance at O/H = 0. Today there is very high signal/noise data on He abundances in approximately 40 metal-poor dwarf irregulars with O/H ranging from 2% to 10% solar, so the extrapolation to O/H = 0 can be estimated to high statistical precision.

The good news is that the best current estimates of Y_p agree to within 5%. This is amazing agreement for measurements derived from spectroscopy of distant galaxies, so we should all feel proud. Nevertheless, the differences in Y_p estimates are a source of consternation for theory of cosmological nucleosynthesis, as the two largest studies obtain values for Y_p which disagree at the 4-5σ significance level: Olive, Skillman & Steigman (1997) derived $Y_p = 0.234 \pm 0.003$, while Izotov & Thuan (1998) derived $Y_p = 0.244 \pm 0.002$ (statistical uncertainties only for both studies), from similar-sized H II region samples. Depending on which estimate is considered most reliable, Y_p either agrees with the best current estimate of D/H under standard Big Bang nucleosynthesis (for $Y_p = 0.244$, or it does not.

At present the battleground for Y_p is focused on sources of systematic error, and these are likely to yield the greatest improvements in He measurements, rather than measuring more data points. The areas that need work are:

- Corrections for He I absorption by the underlying OB association. These are fairly uncertain and affect the He I line ratios as well as the total He abundance. B main sequence and supergiants have the largest He I line strengths, and so need special attention; the B supergiant contribution is likely to be affected by stochasticity and uncertain stellar evolution.
- Density effects. He I lines in the optical spectrum, particularly the triplets, are subject to collisional excitation because the 2 ^{3}S level is metastable. The contribution of collisional excitation depends on both electron density and electron temperature. It is debated whether electron densities typically derived from [S II] line ratios are appropriate for He I. Detailed studies of density structure in a few good H II regions would provide useful information on this.
- Radiative transfer. Again, because the 2 ^{3}S level is metastable, transitions decaying into this level can build up large optical depths in H II regions. This leads to redistribution of line ratios among the triplets. This problem is coupled to the collisional excitation problem.
- Corrections for neutral He. He^0 can not be observed directly in H II regions; the He^0 fraction must be inferred from ionization models. Since the ionization energy of He is 24.6 eV He^0 can exist in the H^+ zone. However, for ionizing radiation field with an effective temperature $T_{eff} > 40{,}000$ K the He^+ Strömgren radius is nearly coincident with the H^+ radius. This problem is largely solved by observing only high-ionization H II regions, with $O^+/O < 0.15$. Nevertheless, even in this case the He^0 corrections can be 1-2%, either positive or negative.
- Collisional excitation of H I. In high temperature metal-poor H II regions, collisional excitation of Hα could be significant (of order 5% or so). H I collisional excitation affects the He/H ratio and interstellar reddening estimates. The effect is very sensitive to the fraction of H^0 present in the highly-ionized zone, which is very uncertain.

Each of these error sources contribute perhaps 1-2% to the uncertainty in derived He abundances, but it is how they sum that determines the systematic error, which is not fully understood.

Helium abundances in spiral galaxies are less well-determined, because of more un-

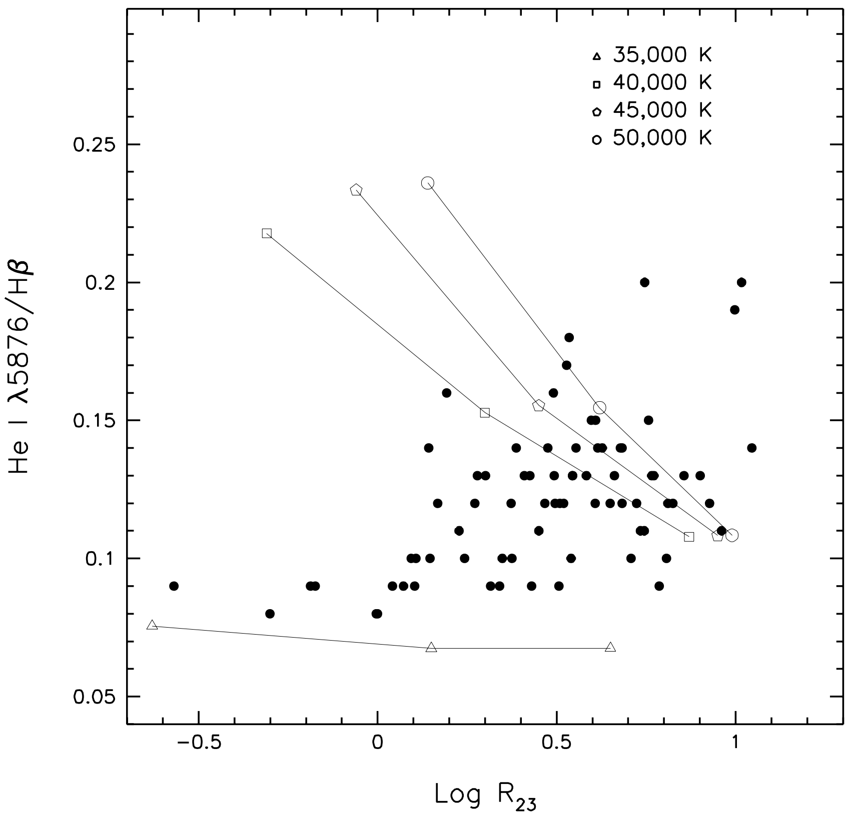

FIGURE 15. I(He I λ5876)/I(Hβ) vs. R_{23} from spectroscopy of H II regions in spiral galaxies (Bresolin et al. 1999), showing how the He I line strengths decrease for low R_{23} (high O/H). Overplotted are trends obtained from photoionization models with various values of T_{eff} for the ionizing stars, assuming that He varies with metallicity as $\Delta Y/\Delta = 2.5$.

certain electron temperatures. The He abundance does have an effect on ionization structure, so it is of interest to know how He/H varies with metallicity in the inner disks of spirals. Does He/H continue to rise linearly with metallicity as in the metal-poor galaxies, or does it level off? This may be difficult to determine from H II region spectroscopy, as there appears to be a drop in the He I line strengths in the inner disks of spirals (Bresolin, Kennicutt, & Garnett 1999), contrary to what one would expect from ionization models with rising or even constant He/H (Figure 15). The low He I 5876 line strengths in the metal-rich regions observed so far are lower than expected even for primordial He/H. The trend of decreasing He I line strength is best explained if ionizing clusters in H II regions with metallicity above solar have radiation fields with characteristic temperatures of about 35,000 K. This is the strongest evidence available for a possible variation in the upper limit of the massive star IMF.

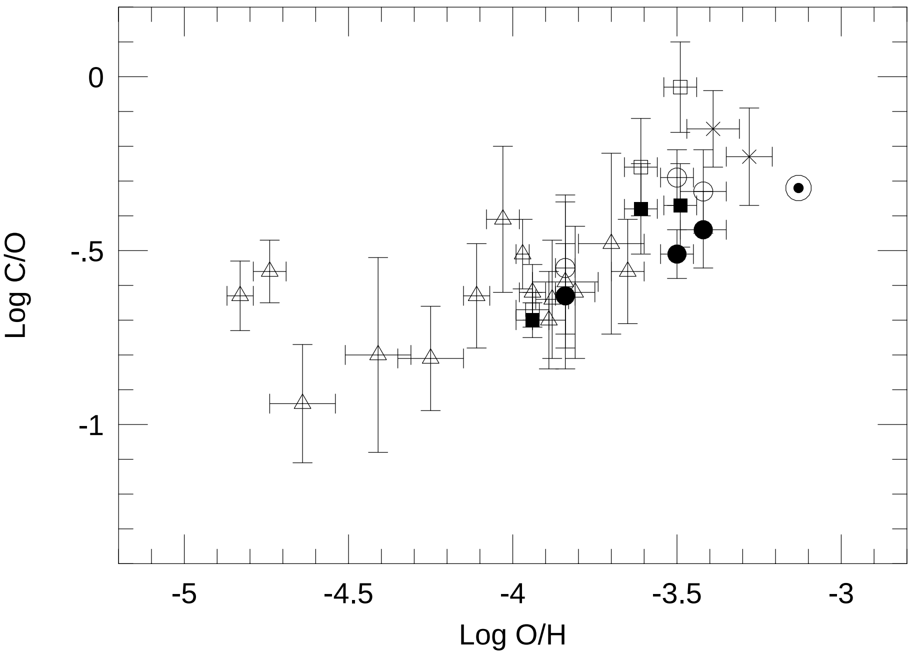

FIGURE 16. C/O abundance ratios (by number) from spectroscopy of H II regions in spiral and irregular galaxies (Garnett et al. 1995a, 1997b, 1999). *Open symbols*: irregular galaxies; *filled symbols*: spiral galaxy H II regions.

5.2. *Carbon*

Carbon abundances in H II regions have been difficult to determine with precision because the important ionization states (C^+, C^{+2}) have no strong forbidden lines in the optical spectrum. Only the UV spectrum shows collisionally excited lines from both C II and C III. A number of studies of carbon abundances in extragalactic H II regions were made with *IUE* (e.g., Dufour, Shields, & Talbot 1982; Peimbert, Peña, & Torres-Peimbert 1986; Dufour, Garnett & Shields 1988), but for the most part the *IUE* observations suffered from low signal/noise and uncertainties due to aperture mismatches between UV and optical spectra.

The higher UV sensitivity of *HST* offered greatly improved measurements of UV emission lines from [C II] and C III], plus the opportunity to scale the C lines directly to [O II] and O III] lines in the UV, tremendously reducing the uncertainties due to reddening corrections and errors in T_e (Garnett et al. 1995a, 1999; Kobulnicky & Skillman 1998). The most recent data for C/O as a function of O/H in dwarf irregular and spiral galaxies from *HST* measurements are displayed in Figure 16. Some C (and O) is expected to be depleted onto interstellar dust grains. Sofia et al. (1997) showed that the gas-phase C abundance varies little with physical conditions in the local neutral ISM, suggesting a constant fraction of C in dust everywhere. They infer that C is depleted by about 0.2 dex. O should be depleted by no more than $\approx$ 0.1 dex everywhere (Mathis 1996). Thus, it is likely that our C/O values should all be increased by 0.1-0.2 dex, but we do not expect any systematic variation in the fractional depletions with metallicity.

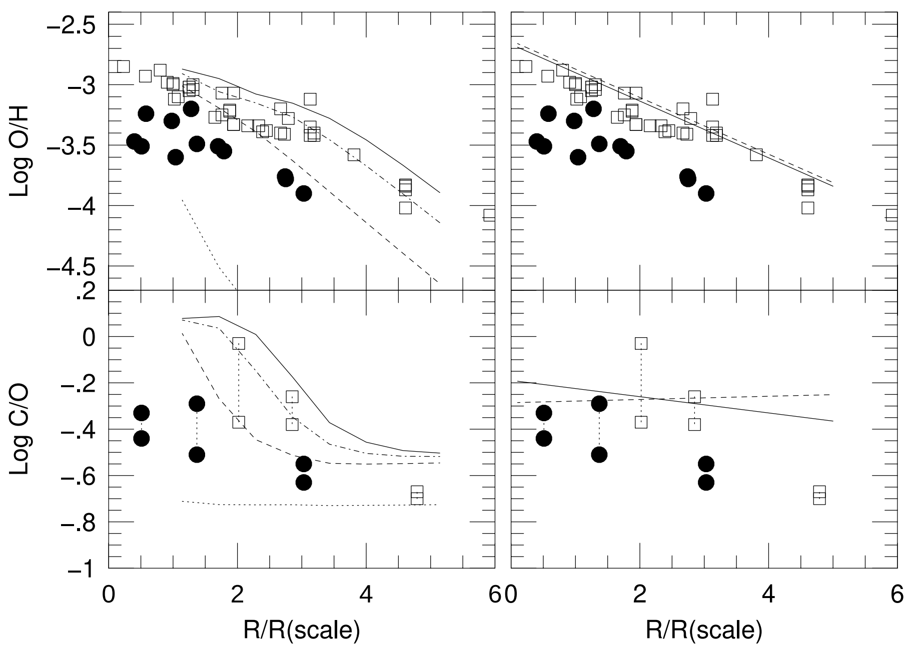

FIGURE 17. C/O and O/H gradients in M101 (open squares) and NGC 2403 (filled circles) plotted vs. radius normalized to the disk scale length (Garnett et al. 1999). *Left panels:* Galactic chemical evolution models from Carigi 1996, using massive star yields from Maeder 1992. The curves show the O/H and C/O gradients at different times, from 0.5 Gyr (*dotted curves*) to 13 Gyr (*solid curves*). *Right panels:* Galactic chemical evolution models from Götz & Köppen 1992 (*dashed line*) and Mollá et al. 1997 (*solid lines*) using massive star yields with no stellar winds. All models use the same intermediate-mass star yields from Renzini & Voli 1981.

Figure 16 shows a trend of steeply increasing C/O for log O/H > -4. This is in agreement with observations of C/O in disk stars in the Galaxy (Gustafsson et al. 1999). The C/O ratios in the most metal-poor galaxies are consistent with the predictions for massive star nucleosynthesis by Weaver & Woosley (1993; hereafter WW93) for their best estimate of the $^{12}C(\alpha,\gamma)^{16}O$ nuclear reaction rate factor. On the other hand, the amount of contamination by C from intermediate mass stars is poorly known in these galaxies.

The notable trend in Figure 16 is the apparent 'secondary' behavior of C with respect to O, despite the fact that C (i.e., ^{12}C) is primary. Tinsley (1979) demonstrated that such variations can be understood as the result of finite stellar lifetimes and delays in the ejection of elements from low- and intermediate-mass stars. If C is produced mainly in intermediate-mass stars, then the enrichment of C in the ISM is delayed with respect to O, which is produced in high-mass stars.

At the same time, C is also produced in high-mass stars, with a production yield that is fairly uncertain. In stars without mass loss, the relative yield of C with respect to O in massive stars is smaller than the solar ratio (WW93), which would demand that most C come from intermediate-mass stars. Maeder (1992), however, showed that stellar mass loss can affect the yields of C and O from massive stars. The effect of such mass loss is to remove He and C from the massive stars before they can be further processed into O. If the mass-loss rates depend on radiative opacity, and thus on metallicity, then the yields of C and O will depend on metallicity, with the C yield increasing with Z at the expense of O.

Figure 17 shows the data for the spiral galaxies M101 and NGC 2403 with the predictions of two sets of chemical evolution models overlaid. The left panels show a sequence of Galactic chemical evolution models using massive star nucleosynthesis models including stellar winds from Maeder (1992); the right panels shows two other Galactic chemical evolution models derived with massive star yields computed assuming no stellar mass loss. All of the models use the same intermediate-mass star yields. Although all of the models reproduce the O/H gradients reasonably well, only the models with Maeder yields seem able to reproduce the steep C/O gradients observed - with the caveat that these models were not tailored for the two galaxies in question. Comparison of solar neighborhood models with the observations of stars also tend to favor the nucleosynthesis models that take into account metallicity-dependent mass loss for massive stars (e.g., Prantzos et al. 1994; Carigi 2000).

The big uncertainties in all of this revolve around the theoretical yields. Problem number one is the $^{12}C(\alpha,\gamma)^{16}O$ reaction rate, which is still highly uncertain (Hale 1998). Problem two is uncertainty in convective mixing. ^{16}O is produced by α captures onto ^{12}C during helium burning. Mixing of fresh He into the convective zone can turn C into O rapidly (Arnett 1996, pp. 223-229). Finally, mass loss rates for stars in various evolutionary states and metallicities are also still uncertain. For intermediate-mass stars, differences in mixing and treatment of thermal pulses affect the C yields. The most recent models for nucleosynthesis in intermediate-mass stars still show large discrepancies in yields (Portinari et al. 1998; van den Hoek & Groenewegen 1997; Marigo et al. 1996, 1998). Until these problems are solved or we have empirically-derived C yields for stars of various masses, it will be difficult to reliably interpret the abundance trends.

5.3. *Nitrogen*

Nitrogen abundances in extragalactic H II regions are almost entirely derived from optical [N II] lines alone, because the other important species, N III, has strong emission lines only in the UV and FIR. Photoionization models generally predict that $N^+/O^+ = N/O$ under most conditions. Nevertheless, IR measurements of [N III]/[O III] in Galactic H II regions consistently find a steeper N/O gradient than that obtained from optical measurements of [N II]/[O II] (Lester et al. 1987; Martín-Hernández et al. 2002). This suggests that ionization corrections may be important (Garnett 1990). Direct comparison between [N II] and [N III] measurements in H II regions with varying properties is needed to understand the nitrogen ionization balance, so that the variation in N with metallicity can be studied accurately. Comparison with measurements in stars is also helpful, and it should be noted that measurements of abundances in B stars (e.g. Rolleston et al. 2000, Korn et al. 2002) yield O and N abundances in good agreement with the values for H II regions in the Milky Way and the LMC and the Local Group spiral M33 (McCarthy et al. 1995; Monteverde et al. 1997).

With this uncertainty in mind, Figure 18 shows how N/O varies with O/H from optical spectroscopy of H II regions in spiral and irregular galaxies. It has been known for some time that N seems to have two components: one component which follows O in a fixed ratio ($\log$ N/O ≈ -1.5) for $\log$ O/H < -3.7, as inferred from the constant N/O vs. O/H in metal-poor dwarf irregular galaxies (open circles), and a second component that increases faster than O at higher O/H as seen in spiral galaxies (filled circles and squares, crosses). The second component is produced via the classical CNO cycle during hydrogen

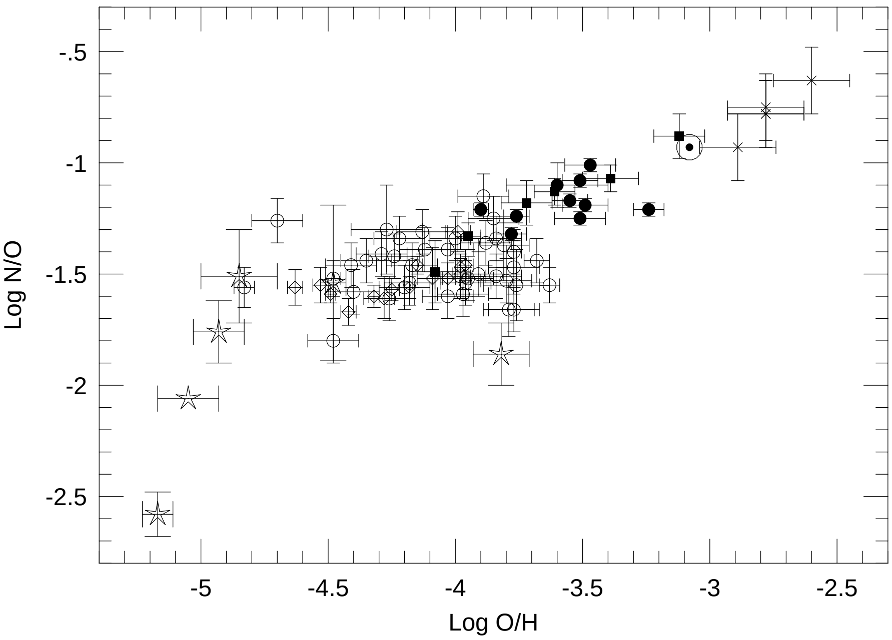

Figure 18. N/O abundance ratios in spiral and irregular galaxies. *Open circles*: Garnett 1990; *open diamonds*: Thuan et al. 1995; *filled circles*: Garnett et al. 1999; *filled squares*: Garnett and Kennicutt 1994, Torres-Peimbert et al. 1989; *plus signs*: Díaz et al. 1991; *stars*: high-redshift absorption line systems from Lu, Sargent, and Barlow 1998. Note the very low N/O in some high-redshift systems.

burning in stars and requires the presence of C and O in the star from birth ("secondary N"), while the first component is postulated to come from the CN cycle on freshly-synthesized C (from He-burning) which has been convectively "dredged-up" into a hot H-burning zone at the base of the convective envelope, and does not require an initial seed of C or O (hence, "primary" N). The latter process is most commonly thought to occur in the asymptotic giant branch (AGB) stage of intermediate mass stars (Iben & Truran 1978), but has been found to occur in models of massive stars with increased convective overshooting or rotationally-induced mixing (e.g. Langer et al. 1997). It has been unclear which primary N source accounts most for the constant N/O in the dwarf galaxies. The massive star primary source does not appear to produce enough N to yield N/O $\approx$ 0.03. For the lower mass stars, the various AGB model calculations give rather discrepant results for the production of N (see Forestini & Charbonnel 1997; van den Hoek & Groenwegen 1997; Marigo 2001). The N production during the third dredge-up is very sensitive to the assumptions that determine the boundary of the convective zone and the overshoot. This is a highly hydrodynamic problem including explosive thermal pulse events and is difficult to model at present (Lattanzio 1998). It is likely that this will continue to be an important topic of study for the near future.

Some insight may be found by examining more distant objects. Recent studies of high-redshift Lyman-alpha absorption systems (plotted as stars in Figure 18) have found

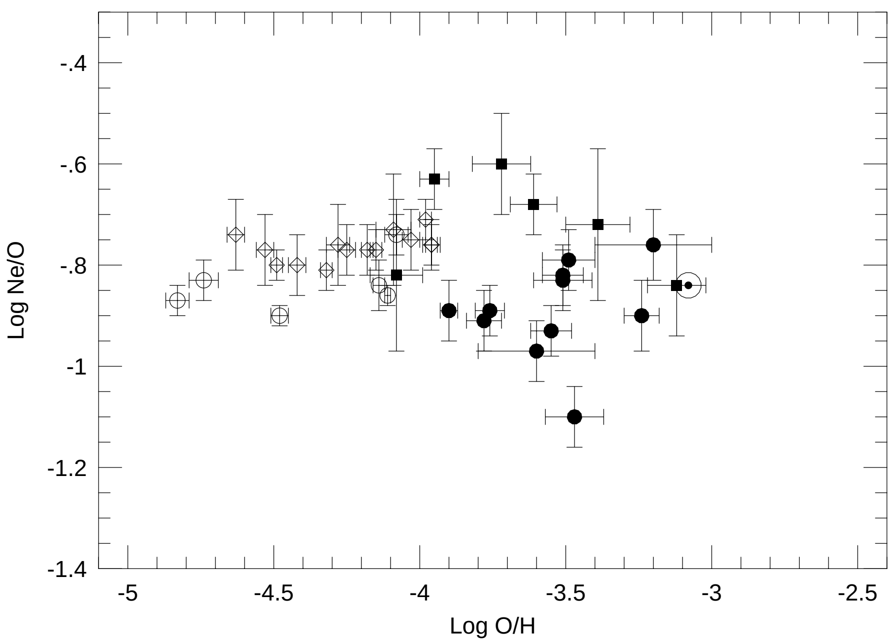

FIGURE 19. Ne/O abundance ratios in spiral and irregular galaxies. Symbols are the same as in Figure 18.

objects with N/S, N/Si, and N/O ratios much lower than in the dwarf galaxies (Pettini, Lipman & Hunstead 1995; Lu, Sargent, and Barlow 1998). A wide range in inferred N/O is seen in the DLAs, but the lowest values are as much as a factor 10 smaller than the average for irregular galaxies. Although S and Si column densities are derived from S II and Si II, which can coexist with both ionized and neutral gas, ionization effects appear to insufficient to account for low N/S and N/Si (Vladilo et al. 2001). The results are consistent with the idea that the DLAs represent lines of sight through very young galaxies, with an age spread of a few hundred Myr, the timescale for enrichment of N from AGB stars. The higher N/O ratios seen in irregular galaxies would then be largely the product of AGB stars.

Some scatter is seen in N/O for the more metal-rich dwarf galaxies (Kobulnicky & Skillman 1998). This may be the result of localized enrichment by Wolf-Rayet stars. The most metal-poor dwarf galaxies seem to show very little scatter in N/O (Thuan et al. 1995). It is possible that this may simply reflect small number statistics (dwarf galaxies with log O/H < -4.5 and bright H II regions are rare). It is also possible to understand these galaxies if they are relatively old systems that experienced an episode of star formation in the past which enriched them to their present composition, and are experiencing a new starburst event after a long quiescent period.

5.4. *Neon, Sulfur and Argon*

Neon, sulfur, and argon are products of the late stages of massive star evolution. ^{20}Ne results from carbon burning, while S and Ar are products of O burning. As they are all considered part of the α-element group, their abundances are expected to track O/H closely.

Neon abundances in extragalactic H II regions are derived primarily from optical measurements of [Ne III], although spacecraft measurements of the IR [Ne II] and [Ne III] fine-structure lines are becoming available. A representative sample of Ne/O values for H II regions with measured T_e in spiral and irregular galaxies is shown in Figure 19. The scatter increases for the H II regions with higher O/H because of the more uncertain electron temperatures. It is apparent that the Ne abundance tracks O quite closely, in agreement with results from planetary nebulae (Henry 1989).

Figure 20 shows data for sulfur and argon. For log O/H < -3.5, S/O and Ar/O are essentially constant with O/H, and fall within the range predicted by WW93. For log O/H > -3.5, however, there is evidence for declining S/O and Ar/O as O/H increases. The cause of the decline is not clear. It is possible that the ionization corrections for unseen S^{+3} have been underestimated in the more metal-rich H II regions. More observational study, especially IR spectroscopy, of metal-rich H II regions is needed, to rule out ionization or excitation effects.

Because S and Ar are produced close to the stellar core, the yields of S and Ar may be sensitive to conditions immediately prior to and during the supernova explosion, such as explosive processing or fall-back onto the compact remnant (WW93). If real, however, the declining S/O and Ar/O cannot be accounted for by simple variations in the stellar mass function and hydrostatic nucleosynthesis (Garnett 1989); some variation in massive star and/or supernova nucleosynthesis at high metallicities (perhaps due to strong stellar mass loss) may be needed.

5.5. *Other Elements*

Few other elements have been measured systematically in extragalactic H II regions, over a wide range of O/H.

Silicon can be measured in H II regions through the UV Si III] doublet at 1883, 1892 Å. Figure 21 shows Si/O measurements from Garnett et al. (1995b) for a small sample of metal-poor galaxies, along with data for several samples of B stars and the Orion nebula. Si/O appears to be roughly constant but smaller than the average for the Sun and the solar neighborhood B stars. Silicon is certainly depleted onto grains in the ISM, and the results in Figure 21 are consistent with a Si depletion of about -0.2 to -0.4 dex in the H II region sample. This is probably appropriate for not very dense, ionized gas (Sofia, Cardelli, & Savage 1994).

Iron has a variety of emission lines from [Fe II] and [Fe III] in the optical spectrum. The [Fe III] 4658 Å is often observed in extragalactic H II regions. Izotov & Thuan (1999) measured [Fe III] in several metal-poor emission-line galaxies and derived Fe abundances. They obtained Fe/O ratios that were similar to the values found for metal-poor stars in the Galactic halo, and used this to argue that the their emission-line galaxies were very young. However, the ionization corrections for Fe are very uncertain, and Fe is highly depleted onto grains in the ISM. If Si is depleted by 0.2 to 0.4 dex, one can use the depletion analysis of Sofia et al. (1994) to estimate that Fe is depleted by about 0.7 to 1.1 dex. It is improbable that O/Fe ratios in H II regions can be used to interpret the enrichment history of the ISM without better understanding of the depletion factors.

6. Open Questions and Concluding Remarks

In conclusion, I'd like to enumerate a few questions regarding the chemical evolution of galaxies that seem to need further investigation.

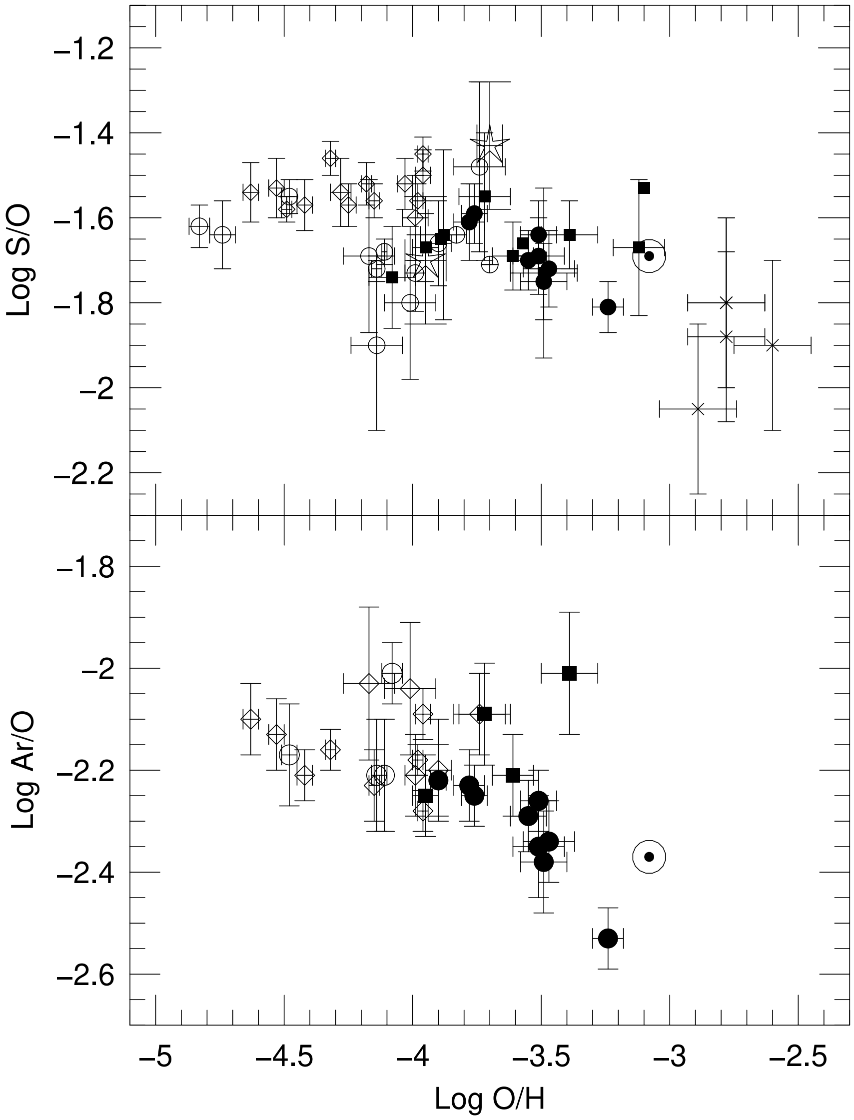

FIGURE 20. *Top:* S/O abundance ratios in spiral and irregular galaxies. *Bottom:* Ar/O abundance ratios in spiral and irregular galaxies. Symbols are the same as in Figure 18.

• What are the primary mechanisms determining the shape and slope of abundance gradients in spiral galaxies? We have seen that chemical evolution models tend to predict that composition gradients should get shallower in the inner disks spirals, but this has not been observed in real galaxies. Does viscous evolution play a role in maintaining an exponential gradient, by transferring new gas into the inner disk? This is essentially

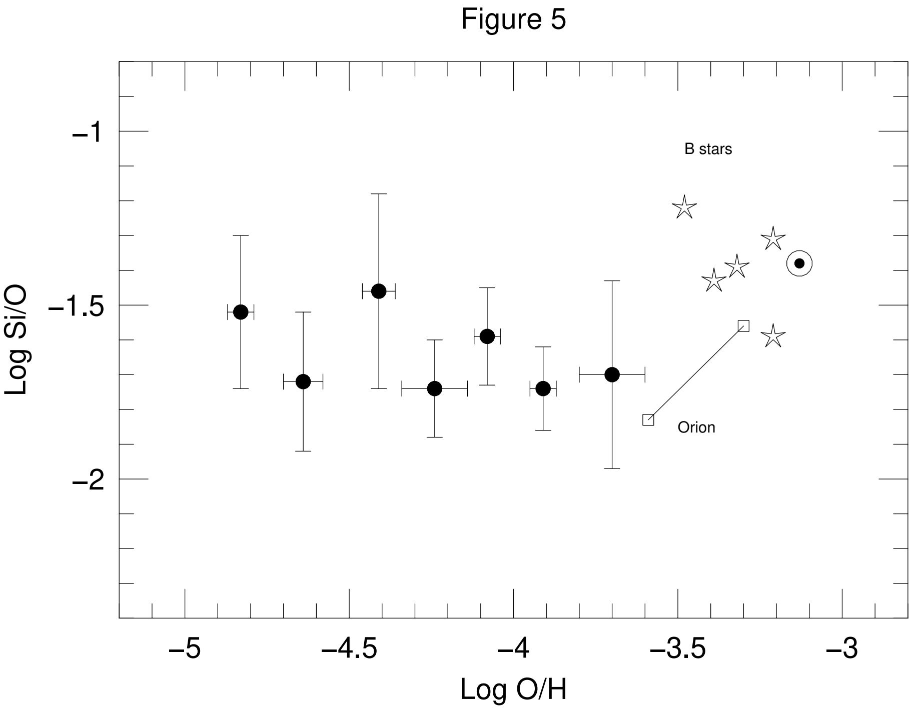

FIGURE 21. Si/O abundance ratios in irregular galaxies, from Garnett et al. 1995b (filled circles). The open squares represent two different measurements for the Orion nebula, while the stars show averages for four samples of Galactic B stars (see Garnett et al. 1995b for details).

a hydrodynamical problem. It is also important to determine how closely composition gradients follow an exponential profile, since the H II region abundance scale is still uncertain for high metallicity. IR spectroscopy will make a significant contribution to constraining the abundance calibrations in the metal-rich regime.

• How homogeneous are abundances in galaxies at a given place and time? Conflicting studies have argued for significant ($\pm$0.2-0.3 dex) variations in abundances on small scales, or for a very homogeneous composition ($<$ 0.1 dex variations). The question is relevant to the time scales for cooling and mixing of stellar ejecta with the ambient ISM. Most chemical evolution models assume instantaneous mixing, but is this a good approximation? Detailed tudies of abundance variations across small ($<$ 1 kpc) regions of galaxies will tell us how homogeneous the ISM composition is.

• Is infall of gas presently occuring in galaxies, and how does the rate evolve with time? This is a big unknown, since most chemical evolution models use relatively slow, ongoing infall of metal-poor gas to suppress the fraction of metal-poor G dwarfs. Observational evidence for classical infall is sketchy. The high-velocity clouds seen at high latitudes may represent infall, or may be part of a Galactic fountain flow, or may be associated with interaction between the Galaxy and its satellite galaxies.

• What galaxies may be losing metals to the IGM, and how much do they contribute? Is there a threshold mass above which galaxies retain metals?

• Does galaxy environment influence composition? The Virgo cluster studies need to be followed up by larger samples in a wider variety of cluster environments. The spiral-rich Ursa Major cluster and the Coma cluster are two obvious choices for continued study.

• Is there zero metallicity gas (or stars for that matter) in galaxies? Pre-enrichment by an initial stellar Population III also provides a solution to the G-dwarf problem and to the origin of metals seen in Lyα forest clouds. What is the composition of the huge gas reservoirs in the outer parts of spirals and irregulars?

For abundance work in ionized nebulae, we need to understand better the effects of dust on the thermal and ionization balance. The calculated ionizing spectra from massive stars are still in a state of flux, as more physics and opacity are included; this is an area that will continue to require attention as computing power grows. The effects of inhomogeneous structure on the observed emission-line spectrum of H II regions also needs to be addressed.

Stellar nucleosynthesis also needs continuing attention. The biggest remaining problem in theoretical stellar evolution and nucleosynthesis continues to be the treatment of convective mixing, which affects both structure and nucleosynthesis. This is also a hydrodynamical problem requiring improved computing power, and should provide a source of entertainment (and argument) for some time.

We are seeing great improvements in the study of abundances in nearby galaxies, particularly with the new space-based UV and IR observatories, which are greatly improving the data for elements besides oxygen. With these new data, we are in a better position to connect the present-day abundance patterns in galaxies with those observed in high-redshift gas clouds. Eventually, emission-line spectroscopy of distant galaxies should greatly expand our information on heavy element abundances at early times, and allow us to trace the evolution of metallicity in the universe in greater detail. This will be an important complement to the absorption line work on DLAs, as the connection between the emission-line gas and the stellar component is much more clear, and the disk component can be sampled more completely than with absorption studies.

For nearby galaxies one challenge for observers is to compile a homogeneous reference set of abundance data, to provide a statisically significant sample for outlining the relationships between abundances, galaxy mass, and Hubble type, and for understanding the effects of environment on abundance profiles. Some Hubble types are poorly represented in the database, particularly very early Hubble types (Sa-Sab), and very late types (Sd). Basic structural data for nearby galaxies also need improvement. The amount and distribution of molecular gas is one area for improvement. Stellar mass-to-light ratios and the stellar mass surface density distribution is another. Wide-field imaging in the infrared should help reduce the uncertainty in the mass of the stellar component.

One might have noticed that many of the theoretical questions mentioned above come down to hydrodynamics. Understanding star formation, the evolution of galaxies, and the structure of stars all involve hydrodynamics at fundamental levels, so I believe that improved hydrodynamical modeling of all of these phenomena will be the key to a better understanding of galaxy evolution. Understanding the mechanisms which connect abundances in galaxies to galaxy structure should provide a continuing challenge to galaxy evolution theorists.

I am grateful to the organizers of this Winter School for the opportunity to meet and interact with the young scientists (on both the galactic and stellar side) whose research papers I have been enjoying in the past couple of years. Special thanks go to Eric Bell for producing Figure 5 for me, and for informative discussions of the properties of galaxy colors and population synthesis models. The review presented here has also benefitted by numerous conversations over the past years with Daniela Calzetti, Mike

Edmunds, Gary Ferland, Claus Leitherer, John Mathis, Andy McWilliam, and Verne Smith. Finally, I must also acknowledge my various collaborators on galaxy abundances (Reginald Dufour, Rob Kennicutt, Greg Shields, Evan Skillman, Manuel Peimbert, and Silvia Torres-Peimbert) who have contributed greatly to many of the results I have presented in these lectures. My work on abundances in galaxies has been supported the past four years by NASA grant NAG5-7734.

REFERENCES

Aller, L. H. & Faulkner, D. J., 1962, PASP 74, 219

Alloin, D., Collin-Soufrin, S., Joly, M., & Vigroux, L., 1979, A&A 78, 200

Anders, E. and Grevesse, N., 1989, Geochim. Cosmochim. Acta 53 197

Andredakis, Y. C., Peletier, R. F., & Balcells, M. 1995, MNRAS 275, 874

Armandroff, T. E. & da Costa, G. S. 1991, AJ 100 1329

Arnett, D., 1996, Supernovae and Nucleosynthesis, (Princeton University Press)

Barnes, J., 1991, IAU Symposium 126, Dynamics of Galaxies and Their Molecular Cloud Distributions, eds. F. Combes and F. Casoli (Dordrecht: Kluwer), 363

Baugh, C. M., Cole, S., & Frenk, C. S., 1996, MNRAS 283, 1361

Bell, E. F., & de Jong, R. S., 2000, MNRAS 312, 497

Bell, E. F., & de Jong, R. S., 2001, ApJ 550, 212

Bosch, G., Terlevich, R., Melnick, J., & Sehman, F., 1999, A&AS 137, 21

Bregman, J. N., Schulman, E., & Tomisaka, K., 1995, ApJ 439, 155

Bresolin, F., Kennicutt, R. C., Jr., & Garnett, D. R., 1999, ApJ 510, 104

Broeils, A. H., 1992, PhD thesis, University of Groningen

Broeils, A. H., & van Woerden, H., 1994, A&AS 107, 129

Burstein, D., Faber, S. M., & González, J. J., 1986, AJ 91, 1130

Calzetti, D., Kinney, A. L., & Storchi-Bergman, T. 1994, ApJ 429, 582

Carigi, L., 1996, RMxAA 32, 179

Carigi, L., 2000, RMxAA 36, 171

Casertano, S., & van Gorkom, J. H., 1991, AJ 101, 1231

Cayatte, V., Kotanyi, C., Balkowski, C., & van Gorkom, J. H., 1994, AJ 107, 1003

Clarke, C. J. 1989, MNRAS, 238, 283

Combes, F., 1998, in Abundance Profiles: Diagnostic Tools for Galaxy History, eds. D. Friedli, M. Edmunds, C. Robert, and L. Drissen (San Francisco: ASP), 300

Combes, F., Debbasch, F., Friedli, D., & Pfenniger, D., 1990, A&A 233, 82

de Koter, A., Heap, S. R., & Hubeny, I., 1997, ApJ, 477, 792

de Jong, R. S. 1996, A&AS, 118, 557

de Vaucouleurs, G., & Pence, W. D., 1978, AJ, 83, 1163

de Zeeuw, P. T., et al., 2002, MNRAS, 329, 513

Dekel, A., & Silk, J. 1986, ApJ, 303, 39

Denicoló, G., Terlevich, R., & Terlevich, E. 2002, MNRAS 330, 695

Díaz, A. I., & Pérez-Montero, E. 2000, MNRAS 312, 130

Díaz, A. I., Terlevich, E., Vílchez, J. M., Pagel, B. E. J., & Edmunds, M. G. 1991, MNRAS 253, 245

Dressler, A. 1980, ApJ, 236, 351

Dufour, R. J., Garnett, D. R., & Shields, G. A., 1988 ApJ 332, 752

Dufour, R. J., Shields, G. A., & Talbot, R. J., Jr. 1982 ApJ 252, 461

EDMUNDS, M. G., 1990, MNRAS, 246, 678

EDMUNDS, M. G., & PAGEL, B. E. J., 1984, MNRAS, 211, 507

EGGEN, O., LYNDEN-BELL, D., & SANDAGE, A., 1962, ApJ, 136, 748

ELLISON, S. L., SONGAILA, S., SCHAYES, J., & PETTINI, M., 1999, AJ, 120, 1175

FERLAND, G. J., 1998, Ringberg Workshop on the Orion Complex (astro-ph/9808107)

FORESTINI, M., & CHARBONNEL, C., 1997 A&AS 123, 241

FRIEDLI, D., BENZ, W., & KENNICUTT, R. C. JR., 1994 ApJ 430, L105

GARNETT, D. R., 1989 ApJ 345, 282

GARNETT, D. R., 1990 ApJ 363, 142

GARNETT, D. R., 1992 AJ 103, 1330

GARNETT, D. R., 1999 in Spectrophotometric Dating of Stars and Galaxies, eds. I. Hubeny, S. Heap, and R. H. Cornett (San Francisco: ASP), 61

GARNETT, D. R., 2002, in preparation

GARNETT, D. R., & DINERSTEIN, H. L., 2001, RMxAASC 10, 13

GARNETT, D. R., & DINERSTEIN, H. L., 2002, ApJ 558, 145

GARNETT, D. R., DUFOUR, R. J., PEIMBERT, M., TORRES-PEIMBERT, S., SHIELDS, G. A., SKILLMAN, E. D., TERLEVICH, E., & TERLEVICH, R. J.,, 1995b, ApJ 449, L77

GARNETT, D. R., & KENNICUTT, R. C. JR., 1994, ApJ 426, 123

GARNETT, D. R., KENNICUTT, R. C. JR., CHU, Y.-H., & SKILLMAN, E. D. 1991, ApJ 373, 458

GARNETT, D. R., & SHIELDS, G. A., 1987, ApJ, 317, 82

GARNETT, D. R., SHIELDS, G. A., SKILLMAN, E. D., SAGAN, S. P., AND DUFOUR, R. J., 1997a, ApJ 489, 63

GARNETT, D. R., SHIELDS, G. A., PEIMBERT, M., TORRES-PEIMBERT, S., SKILLMAN, E. D., DUFOUR, R. J., TERLEVICH, E., AND TERLEVICH, R. J., 1999, ApJ 513, 168

GARNETT, D. R., SKILLMAN, E. D., DUFOUR, R. J., PEIMBERT, M., TORRES-PEIMBERT, S., TERLEVICH, E., TERLEVICH, R. J., AND SHIELDS, G. A., 1995a, ApJ 443, 142

GARNETT, D. R., SKILLMAN, E. D., DUFOUR, R. J., AND SHIELDS, G. A., 1997b, ApJ 481, 174

GÖTZ, M., & KÖPPEN, J., 1992 A&A 260, 455

GUNN, J. E., & GOTT, J. R., 1972 ApJ 176, 1

GUSTAFSSON, B., KARLSSON, T., OLSSON, E., EDVARDSSON, B., AND RYDE, N., 1999, A&A 342, 426

HALE, G. M. 1998, Stellar Evolution, Stellar Explosions, and Galactic Chemical Evolution, ed. A. Mezzacappa (Bristol: Institute of Physics), 17

HASAN, H., PFENNIGER, D., & NORMAN, C. 1993, ApJ 409, 91

HENRY, R. B. C. 1989, MNRAS 241, 453

HENRY, R. B. C., BALKOWSKI, C., CAYATTE, V., EDMUNDS, M. G., & PAGEL, B. E. J. 1996, MNRAS 293, 635

HENRY, R. B. C., PAGEL, B. E. J., & CHINCARINI, G. L. 1994, MNRAS 266, 421

HENRY, R. B. C., & WORTHEY, G. 1999, PASP 111, 919

HUNTER D. A., BAUM, W. A., O'NEIL, E. J., JR., & LYNDS, R. 1996, ApJ 456, 174

HUNTER D. A., SHAYA, E. J., HOLTZMAN, J. A., LIGHT, R. M., O'NEIL, E. J. JR., & LYNDS, R. 1995, ApJ 448, 179

IBATA, R. A., GILMORE, G., & IRWIN, M. J. 1994 Nature 370, 194

IBEN, I. JR., AND TRURAN, J. W. JR., 1978 ApJ 220, 980

ISRAEL, F. P., 1997a A&A 317, 65

ISRAEL, F. P., 1997b A&A 328, 471

Izotov, Y. I., & Thuan, T. X., 1998 ApJ 500, 188

Izotov, Y. I., & Thuan, T. X., 1999 ApJ 511, 639

Jablonka, P., Martin, P, & Arimoto, N. 1996, AJ 112, 1415

Jacoby, G. H., & Ciardullo, R. 1999, ApJ 515, 169

Kauffmann, G., 1996, MNRAS, 281, 475

Kenney, J. D. P., & Young, J. S., 1989, ApJ, 344, 171

Kennicutt, R. C., Jr., and Garnett, D. R., 1996, ApJ, 456, 504

Kobulnicky, H. A., & Skillman, E. D., 1996, ApJ, 471, 211

Kobulnicky, H. A., & Skillman, E. D., 1998, ApJ, 497, 601

Korn, A. J., Keller, S. C., Kaufer, A., Langer, N., Przybilla, N., Stahl, O., & Wolf, B., 2002, A&A, in press (astro-ph/0201453)

Langer, N., Fliegner, J., Heger, A., and Woosley, S. E., 1997 Nucl. Phys. A621, 457

Lattanzio, J. C. 1998, Stellar Evolution, Stellar Explosions, and Galactic Chemical Evolution, ed. A. Mezzacappa (Bristol: Institute of Physics), 299

Lester, D. F., Dinerstein, H. L., Werner, M. W., Watson, D. M., Genzel, R. L., & Storey, J. W. V., 1987 ApJ 320, 573

Lequeux, J., Rayo, J. F., Serrano, A., Peimbert, M., & Torres-Peimbert, S., 1979 A&A 80, 155

Lin, D. N. C., & Pringle, J. E., 1987, ApJ, 320, L87

Liu, X.-W., Storey, P. J., Barlow, M. J., & Clegg, R. E. S. 1995, MNRAS 272, 369

Liu, X.-W., Storey, P. J., Barlow, M. J., Danziger, I. J., Cohen, M., & Bryce, M. 2000, MNRAS 312, 585

Lu, L., Sargent, W. L. W., and Barlow, T. A., 1998 AJ 115, 55

Maeder, A., 1992 A&A 264, 105

Maloney, P., & Black, J. H., 1988, ApJ, 389, 401

Marigo, P., 2001, A&A, 370, 194

Marigo, P., Bressan, A., & Chiosi, C., 1996, A&A, 313, 545

Marigo, P., Bressan, A., & Chiosi, C., 1998, A&A, 331, 580

Martin, P. G., & Rouleau, F., 1990, in Extreme Ultraviolet Astronomy, eds. R. F. Malina and S. Bowyer (Oxford: Pergamon), 341

Martin, P., & Roy, J.-R., 1994, ApJ, 424, 599

Martín-Hernández, N. L., Peeters, E., et al. 2002, A&A, 381, 606

Martins, F., Schaerer, D., & Hiller, D. J. 2002, A&A 382, 999

Mateo, M., 1998, ARAA 36, 435

Mathis, J. S., 1962, ApJ 136, 374

Mathis, J. S., 1996, ApJ 472, 643

Matteucci, F., and Chiosi, C., 1983 MNRAS 239, 885

Matteucci, F., and François, P., 1989 MNRAS 239, 885

McCall, M. L., 1982, PhD thesis, University of Texas at Austin

McCarthy, J. K., Lennon, D. J., Venn, K. A., Kudritzki, R.-P., Puls, J., & Najarro, F., 1995, ApJ 455, L135

McWilliam, A. & Rich, R. M., 1994, ApJS 91, 749

Mighell, K. J. & Burke, C. J., 1999, AJ 118, 366

Mihos, J. C., 2001, in Galaxy Disks and Disk Galaxies, ASP Conference Series Vol. 230, eds. J. G. Funes and E. M. Corsini, p. 491

Mo, H., Mao, S., & White, S. D. M., 1998, MNRAS, 295, 319

Mollá, M., Ferrini, F., & Díaz, A. I., 1997, ApJ, 475, 519

Monteverde, M. I., Herrero, A., Lennon, D. J., & Kudritzki, R.-P., 1997, ApJ, 474, 107

Oey, M. S., & Kennicutt, R. C. Jr. 1993 ApJ 411, 137

Osterbrock, D. E. 1989, Astrophysics of Gaseous Nebulae and Active Galactic Nuclei (Mills Valley, CA: University Science Books)

Olive, K. A., Skillman, E. D., & Steigman, G., 1997 ApJ 483, 788

Pagel, B. E. J., Edmunds, M. G., Blackwell, D. E., Chun, M. S., & Smith, G., 1979, MNRAS 189, 95

Pakull, M. W., & Angebault, L. P., 1986, Nature 322, 511

Peimbert, M., Peña, M., & Torres-Peimbert, S., 1986 A&A 158, 266

Peimbert, M., & Spinrad, H., 1970 ApJ 159, 809

Peimbert, M., & Torres-Peimbert, S., 1974 ApJ 193, 327

Pelletier, R. F., et al. 1999, MNRAS, 310, 863

Pettini, M., Lipman, K., and Hunstead, R. W., 1995, ApJ, 451, 100

Phillips, S., & Edmunds, M. G., 1991, MNRAS, 251, 84

Portinari, L., Chiosi, C., & Bressan, A., 1998, A&A 334, 505

Prantzos, N., & Boissier, S., 2000, MNRAS, 313, 338

Prantzos, N., Vangioni-Flam, R., & Chauveau, S., 1994, A&A, 285, 132

Renzini, A., & Voli, M., 1981, A&A 94, 175

Rich, R. M., & McWilliam, A., 2000, Proc. SPIE 4005, 150

Rolleston, W. R. J., Smartt, S. J., Dufton, P. L., & Ryans, R. S. I., 2000, A&A 363, 537

Roy, J.-R.., & Walsh, J. R., 1997, MNRAS, 288, 715

Rudnick, G., & Rix, H.-W., 1998, AJ, 116, 1163

Ryder, S. D., 1995, ApJ, 444, 610

Searle, L., 1971, ApJ, 168, 327

Searle, L., & Sargent, W. L. W., 1972, ApJ, 173, 25

Searle, L., & Zinn, R., 1978, ApJ, 225, 357

Shetrone, M. D., Coté, P., & Sargent, W. L. W., 2001, ApJ, 548, 592

Shields, J. C., & Kennicutt, R. C. Jr., 1995, ApJ, 454, 807

Skillman, E. D., 1998, Stellar Astrophysics for the Local Group, eds. A. Aparicio, A. Herrero, and F. Sánchez (Cambridge University Press), 457

Skillman, E. D., & Bender, R., 1995, RMxAASC, 3, 25

Skillman, E. D., Kennicutt, R. C., Jr., Shields, G. A., & Zaritsky, D., 1996, ApJ, 462, 147

Smecker-Hane, T. A., Stetson, P. B., Hesser, J. E., & Lehnert, M. D., 1994 AJ 108, 507

Sneden, C., Cowan, J. J, Ivans, I. I., Fuller, G. M., Burles, S., Beers, T. C., & Lawler, J. E., 2000 ApJ 533, L139

Sofia, U. J., Cardelli, J. A, Guerin, K. P., and Meyer, D. M., 1997 ApJ 482, L105

Sofia, U. J., Cardelli, J. A, & Savage, B. D., 1994 ApJ 430, 650

Stasińska, G., & Szczerba, G. P., 2001, A&A 379, 1024

Tayal, S. S., & Gupta, G. P., 1999 ApJ 526, 544

Thuan, T. X., Izotov, Y. I., and Lipovetsky, V. A., 1995 ApJ 445, 108

Tinsley, B. M., 1979 ApJ 229, 1046

Tolstoy, E., Irwin, M. J., Cole, A. A., Pasquini, L., Gilmozzi, R., & Gallagher, J. S., 2001 MNRAS 327, 918

Torres-Peimbert, S., Peimbert, M. and Fierro, J., 1989 ApJ 345, 186

Trager, S. C., Faber, S. M., Worthey, G., & González, J. J., 2000a, AJ 119, 1645

Trager, S. C., Faber, S. M., Worthey, G., & González, J. J., 2000b, AJ 120, 165

Tsujimoto, T., Yoshii, Y., Nomoto, K. and Shigeyama, T., 1995 A&A 302, 704

Tyson, J. A., 1986 J. Opt. Soc. Amer. A 3, 2131

van den Hoek, L. B., & Groenewegen, M. A. T., 1997 A&AS 123, 305

van Zee, L., Salzer, J., Haynes, M., O'Donoghue, A. & Balonek, T., 1998 AJ 116, 2805

Vila-Costas, M. B., & Edmunds, M. G., 1992, MNRAS, 259, 121 (VCE)

Vladilo, G., Centurión, M., Bonifacio, P. & Howk, J. C., 2001 ApJ 557, 1007

Walborn, N. R. 1991, IAU Symposium 148: The Magellanic Clouds, eds. R. Haynes and D. Milne (Dordrecht: Kluwers), 145

Warmels, R. H. 1988, A&AS 72, 427

Weaver, T. A., & Woosley, S. E., 1993 Phys. Rep. 227, 65 (WW93)

Whiting, A. B., Hau, G. K. T., & Irwin, M. J., 1999 AJ 118, 2767

Wilson, C. D. 1995 ApJ 448, L97

Worthey, G. 1998 PASP 110, 888

Yun, M. S., Ho, P. T. P., & Lo, K. Y., 1994 Naturee 372, 530

Zaritsky, D., 1995, ApJ, 448, L17

Zaritsky, D., Kennicutt, R. C. Jr., & Huchra, J. P., 1994, ApJ, 420, 87 (ZKH)